CANADIAN THESES

THÈSES CANADIENNES

NOTICE

The quality of this microfiche is heavily dependent upon the quality of the original thesis submitted for microfilming. Every effort has been made to ensure the highest quality of reproduction possible.

If pages are missing, contact the university which granted the degree.

Some pages may have indistinct print especially if the original pages were typed with a poor typewriter ribbon or if the university sent us an inferior photocopy.

Previously copyrighted materials (journal articles, published tests, etc.) are not filmed.

Reproduction in full or in part of this film is governed by the Canadian Copyright Act, R.S.C. 1970, c. C-30.

AVIS

La qualité de cette microfiche dépend grandement de la qualité de la thèse soumise au microfilmage. Nous avons tout fait pour assurer une qualité supérieure de reproduction.

S'il manque des pages, veuillez communiquer avec l'université qui a conféré le grade.

La qualité d'impression de certaines pages peut laisser à désirer, surtout si les pages originales ont été dactylographiées à l'aide d'un ruban usé ou si l'université nous a fait parvenir une photocopie de qualité inférieure.

Les documents qui font déjà l'objet d'un droit d'auteur (articles de revue, examens publiés, etc.) ne sont pas microfilmés.

La reproduction, même partielle, de ce microfilm est soumise à la Loi canadienne sur le droit d'auteur, SRC 1970, c. C-30.

THIS DISSERTATION HAS BEEN MICROFILMED EXACTLY AS RECEIVED

LA THÈSE A ÉTÉ MICROFILMÉE TELLE QUE NOUS L'AVONS REÇUE

STATISTICAL ANALYSIS OF THE PARTIAL BLEACHING METHOD OF THERMOLUMINESCENCE DATING OF SEDIMENTARY ROCK

by

JEN-NI KUO

B.Sc.(Chemistry), University of British Columbia, 1981

PROJECT SUBMITTED IN PARTIAL FULFILLMENT OF

THE REQUIREMENTS FOR THE DEGREE OF

MASTER OF SCIENCE

in the Department

of

Mathematics and Statistics

SIMON FRASER UNIVERSITY

July 1986

ISBN 0-315-36321-5

APPROVAL

Name: JEN-NI KUO

Degree: Master of Science

Title of project: STATISTICAL ANALYSIS OF THE PARTIAL BLEACHING METHOD OF THERMOLUMINESCENCE DATING OF SEDIMENTARY ROCK

Examining Committee:

Chairman: Dr. A.R. Freedman

Dr. R.A. Lockhart
Senior Supervisor

Dr. D. Eaves

Dr. R.D. Routledge

Dr. R. Cheng
External Examiner
Visiting Associate Professor
Department of Mathematics and Statistics
Simon Fraser University

Date Approved: June 13th, 1986

PARTIAL COPYRIGHT LICENSE

I hereby grant to Simon Fraser University the right to lend my thesis, project or extended essay (the title of which is shown below) to users of the Simon Fraser University Library, and to make partial or single copies only for such users or in response to a request from the library of any other university, or other educational institution, on its own behalf or for one of its users. I further agree that permission for multiple copying of this work for scholarly purposes may be granted by me or the Dean of Graduate Studies. It is understood that copying or publication of this work for financial gain shall not be allowed without my written permission.

Title of Thesis/Project/Extended Essay

Statistical Analysis of the Partial Bleaching Method of Thermoluminescence Dating of Sedimentary Rock

Author: _____
(signature)

Jen-ni Kuo
(name)

July 15, 1986
(date)

ABSTRACT

The statistical analysis of the partial bleaching method of thermoluminescence dating of sedimentary rock is studied. Large sample theory is given for three methods of fitting saturating exponential additive dose curves when the errors are assumed to have a standard deviation proportional to the true response. The three methods, non-linear least squares, maximum likelihood and iteratively reweighted least squares, are shown to be approximately equivalent in the limit of small errors. Approximate standard errors are provided for the intersection point of two such curves. The quality of these approximations is studied by Monte Carlo and shown to be adequate for typical experimental situations. Finally, the techniques are applied to several data sets and the model assumptions are checked informally.

DEDICATION

To my dear parents

Dr. and Mrs. Kuo

with love...

ACKNOWLEDGEMENTS

I would like to thank my supervisory committee for their helpful suggestions in producing this work. Particularly, my sincere thanks to Dr. Richard Lockhart for his major contribution of project ideas, his invaluable guidance and his helpful assistance with the technical difficulties I encountered during the preparation of this project.

I extend my most sincere thanks to my friend, Daniel Stroh, for his support and encouragement throughout the course of my studies and the great help he gave to me in preparing this project and presentation.

TABLE OF CONTENTS

LIST OF TABLES

LIST OF FIGURES

INTRODUCTION

Thermoluminescence (TL) is the phenomenon of the release of visible photons by thermal means. This behaviour was first reported by Boyle about 300 years ago. By the early 1900s, thermoluminescence was well recognized. In 1950, Daniels proposed the application of TL in radiation dosimetry and in 1961, Johnson applied this phenomenon to determine the age of lava flows. To date, thermoluminescence has been applied to a variety of studies including radiation dosimetry, geological age determination, archaeology, climate and paleotemperature studies as well as meteorite and lunar luminescence. In geology, for example, thermoluminescence dating techniques have benefitted research in glacialacustrine silts and marine sediments.

Thermoluminescence dating of sediments was first recognized by G.V. Morzov and V.N. Shelkoplyas. Unfortunately, because researchers at that time were not aware of problems such as the lower sensitivity to alpha particles and the effect of oxygen if the sample was heated in air, early attempts to date rocks produced meaningless ages. During these early years Bothner and Johnson (1969) reported their TL studies on four deep-sea cores rich in foraminifera, but new TL studies of sedimentary deposits were not reported until as late as 1976 by Huntley and Johnson. In 1982, Wintle and Huntley applied thermoluminescence techniques to the dating of the deposition of Quaternary sediments from their last exposure to sunlight. These Quaternary

sediments were deposited approximately two million years ago due to dramatic climatic changes.

Fundamentally, the general procedure is as follows:

Sedimentary rocks are excavated in such a way as to prevent exposure to sunlight. As a precaution all further experiments are carried out under subdued orange light and the sample's outer layers are removed. The sample is then treated to a series of filtrations, acidification and oxidizing steps, and washings in order to remove debris, carbonates and other organic materials, minerals and mineral oxide layers. The resulting slurry is treated with chemical (oxides) and mechanical dispersing mechanisms, to arrive at a number of uniform sample suspensions which are then dried on aluminum discs. Each aluminum disc holds one subsample which weighs approximately 1 milligram. These subsamples (10 to 20) are irradiated with different doses of gamma (γ) radiation. This radiation is thought of as acting in addition to radiation which has irradiated the rock since the rock's last exposure to sunlight. (Exposure to sunlight drives off the trapped electrons and zeroes the TL signal.) Each subsample is then placed into an oven separately.

The TL intensities from room temperature to about 500°C are collected from a photomultiplier tube which is connected to an oven containing an oxygen-free gas at a pressure of less than 1 Pa. TL intensities are then plotted against the corresponding

temperatures at which the TL emitted is observed. This TL versus temperature curve is called the 'glow curve'. Both the Natural TL (NTL) versus temperature and the TL versus temperature curves are glow curves. The NTL signal is the thermoluminescence released by dose-free sediment samples, while the TL signal is the thermoluminescence induced from laboratory irradiated sediment samples (samples bombarded by γ radiation). From a resulting glow curve a single TL value at some high temperature (above ~250°C) is chosen. This high temperature is chosen because TL signal becomes unstable at a temperature lower than 250°C. For any fixed high temperature a plot of TL versus added Co-60γ dose is possible. This plot is called an Additive Dose curve. The diagram on the following page shows a plot of TL versus added dose at a given temperature.

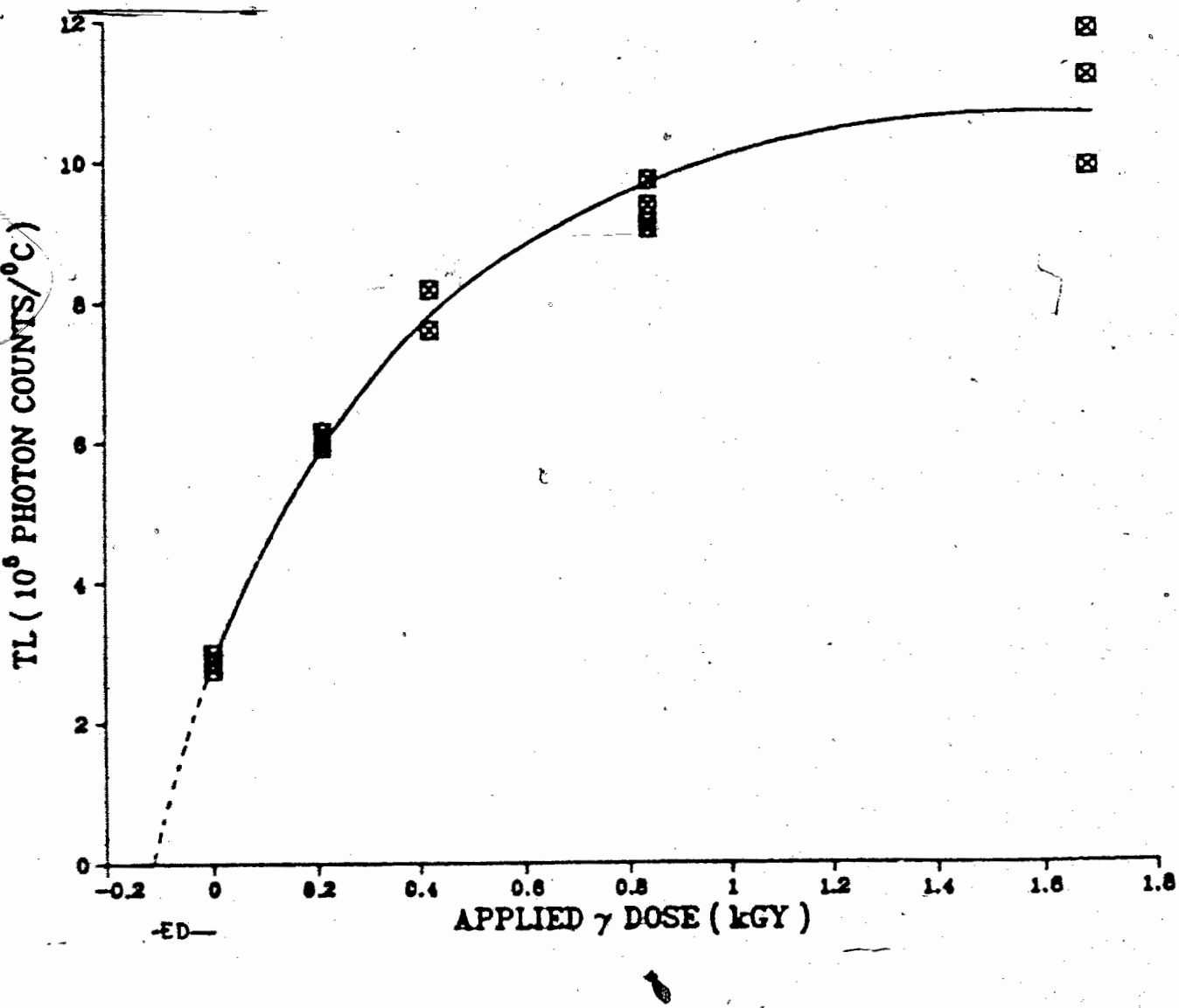

[Figure 0.1] TL versus Added Dose at a given temperature.
A single additive dose curve is shown in this diagram. The ED is the distance from origin to the intercept of the curve and the Applied Dose axis (x-axis).

Extrapolation back to the point of intersection with the Applied Dose axis (x-axis) gives the equivalent dose, ED (or Deq). Several such curves produce ED values which, when plotted with temperature, increase until a plateau is reached. The desired ED, therefore, is the ED for the temperature at which no further change is observed with increasing temperature. An improved method of dating sedimentary rocks introduced by Wintle and Huntley in 1980 is called the partial-bleach or R-GAMMA (R-Γ) procedure. The R-Γ procedure is so named because the reduction (R) in the TL caused by bleaching the unirradiated and the irradiated sedimentary subsamples is plotted against the applied gamma (Γ) dose. The ED is then evaluated from the intersection of bleached and unbleached additive dose curves. 'Bleaching' is a means of reducing the TL due to the radiation dose since deposition by placing the sample under a sun lamp for some length of time. More bleaching produces a larger ED, but not significantly larger when compared to the Standard Error (SE) of the intersection point if the sample was properly zeroed. (Experimental results are shown in Table 5.2.) The plots on the following two pages show the intersection points between the bleached and unbleached additive dose curves, and their equivalent doses at a given temperature.

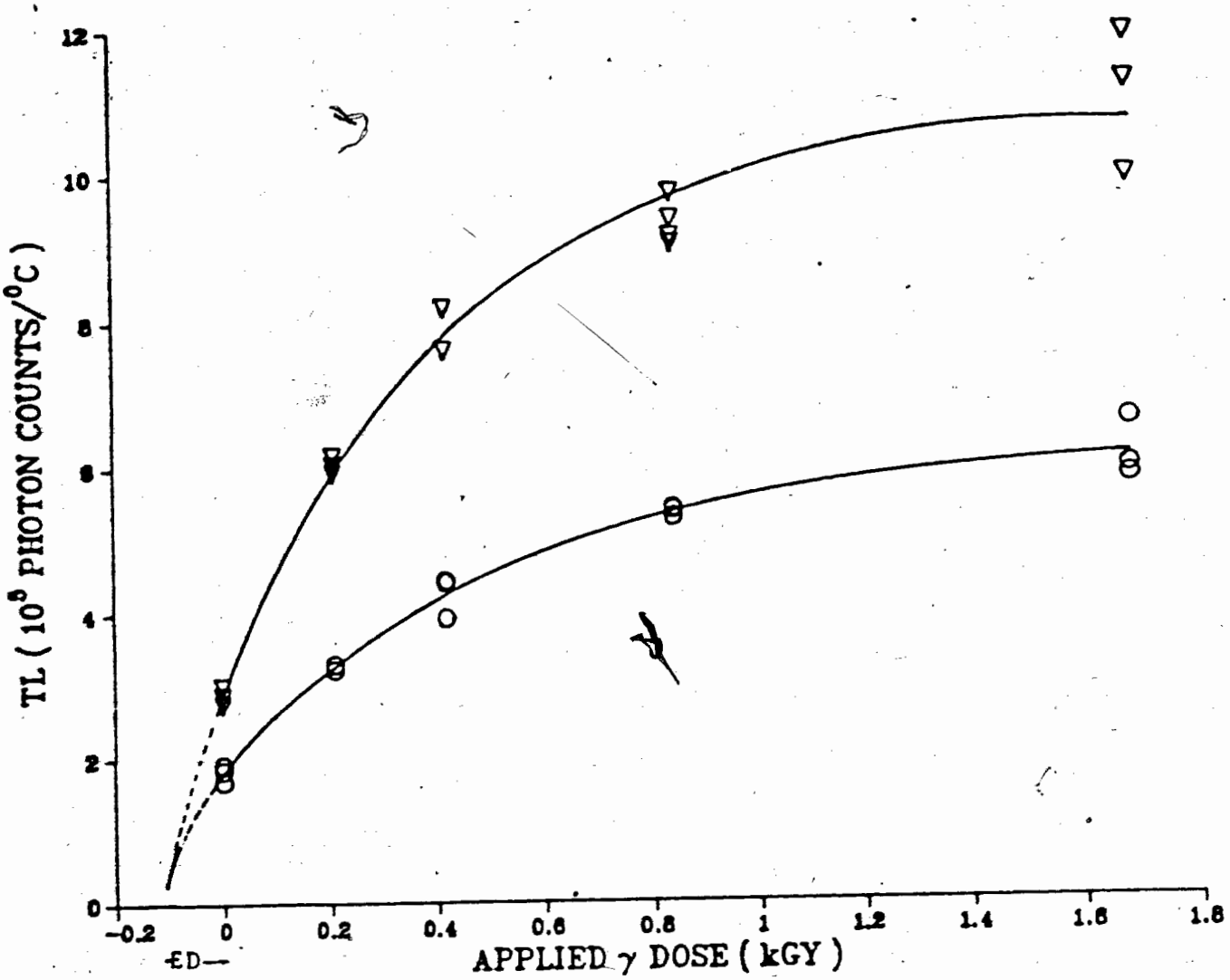

[Figure 0.2] TL versus Added Dose at a given temperature.
Two additive dose curves are shown on this diagram. Both TL signals are induced from γ dose irradiation . The upper figure is the unbleached curve; and the lower is the bleached curve. The ED is the distance from origin to the intersection of these two TL response curves.

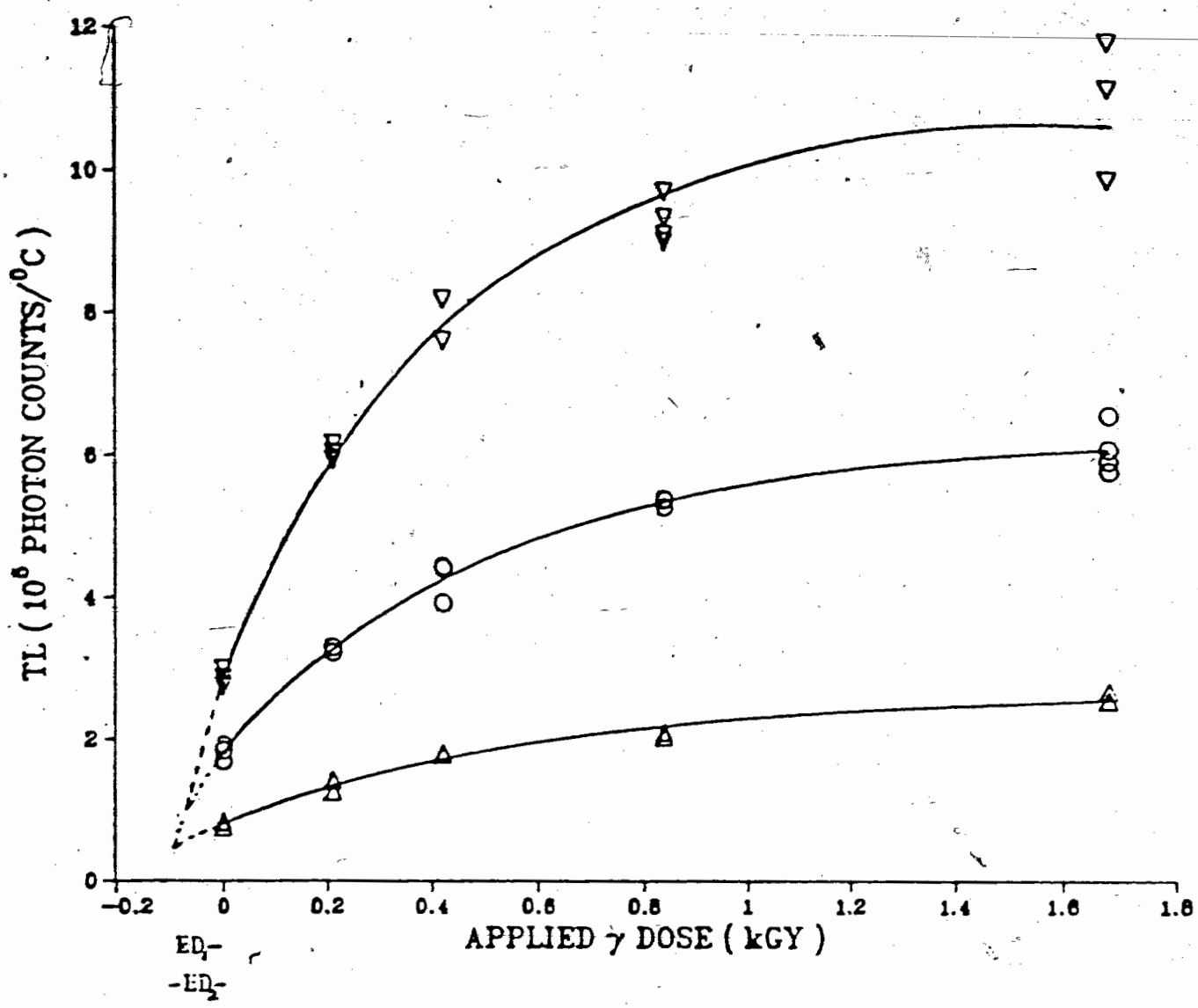

[Figure 0.3] TL versus Added Dose at a given temperature.

Three additive dose curves are shown in this diagram. All TL signals are induced from laboratory γ irradiation. The uppermost figure is the unbleached curve; the middle figure is the bleached curve; and the lower is the bleached curve which represents a sample exposed to a sun lamp for a longer period of time than the bleached curve of the middle figure. There are two EDs are observed. ED_1 is the equivalent dose resulting from the intersection of the unbleached curve and the bleached curve of the middle figure while ED_2 is the equivalent dose resulting from the intersection of the unbleached curve and the bleached curve of the lower figure. Both EDs are the distances from origin to the intersections of the unbleached and the bleached curves.

The desired ED is then applied to the TL apparent age equation as follows:

TL Apparent Age = Equivalent Dose / Effective Dose Rate,

where the Effective Dose Rate is the gamma dose rate applied by cosmic rays to the sedimentary subsamples after accounting for the decay of naturally occuring radioactive isotopes U-238, Th-232 and K-40 in the sediments. The age of the sediment is thereby estimated.

Even though dating of unheated Quaternary sediments has offered the promise of accurate results, some characteristics inherent in the experimental data (elucidated in Chapter One) make relatively simple statistical analysis inappropriate. It is therefore the purpose of this paper to study appropriate statistical analysis of thermoluminescence based on experimental results from the partial-bleach or R-Γ procedure.

For the R-Γ procedure the fundamental problem in estimating the TL apparent age is to accurately extrapolate to the intersection point of two non-linear additive dose curves and to estimate the associated uncertainty. In order to solve this problem the appropriate statistical analysis is discussed in the following Chapters. Chapter One of this paper will outline possible models for means, such as: Linear, Quadratic, Cubic and Exponential models, as well as possible models for the errors. Chapter Two will examine three methods of estimating parameters (coefficients) of the proposed saturating exponential model:

section 2.1.1, Non-Linear Least Squares method; section 2.1.2, Maximum Likelihood method and section 2.1.3, Iteratively Reweighted Least Squares method. In Chapter Three an accurate extrapolation method for the intersection points of unbleached and bleached TL response curves is described. A Maximum Likelihood technique is applied to the estimation of the variances (uncertainties) of these intersection points. In Chapter Four a Monte Carlo Simulation will serve to check the validity of the theories of estimating the parameters and the intersection points and their associated variances as discussed in Chapters Two and Three. Chapter Five uses actual experimental data to fit the proposed model and analyze the methods of estimating the parameters and variances of the intersection points described above. As well, the model assumptions are checked informally. Another method of fitting additive dose curves is suggested in Chapter Six.

CHAPTER 1

POSSIBLE MODELS FOR MEANS AND ERRORS

In section 1.1 and section 1.2 of this Chapter the models for means and errors will be described, respectively. In each of these two sections various possible models will be illustrated. As well the reasons for using the saturating exponential model for the mean and assuming a constant percent error (unknown in advance) for the proposed model will be explained.

1.1 POSSIBLE MODELS FOR MEANS

For sediments younger than 10-20 kiloyears (Ka) the two TL response curves appear linear. This straight-line behaviour makes the simple least-squares method possible for statistical analysis of the data. The straight-line, least-squares fit for young marine sediments has been discussed by Berger et al. (1984).

For sediments older than 20 Ka, dose response curves are no longer linear but sublinear. Sublinear curves show a linear relationship with a positive slope between TL and the applied dose at low dose levels but curvature is observed as the dose level increases and finally a flat TL intensity is reached at a high dose level. There are several possible curves to describe this nonlinearity. Low degree polynomials such as Quadratic and Cubic are linear in their coefficients and empirically fit the data better at the linear portion (low dose levels) than at the

curved portion of the data but as of yet no physical explanation accounts for this. The Quadratic and Cubic models were fitted to the data and discussed by Berger et al. (1985). For very old sediments (older than several hundred thousand years) or at very high applied dose levels (greater than several thousand Gray, kGy; 1 Gray is the S.I. unit for absorbed dose of ionizing radiation) a more physically realistic model is the non-linear saturating exponential model (Huntley et al. 1985). This model is proposed for the following two reasons:

[1] The electron traps contributing to the TL signal become filled.

[2] The physical characteristics of the data suggest a saturating exponential curve.

This model may be written (for a particular temperature) as follows:

$$Y_i = a + b*\exp(-cx_i) + \epsilon_i \qquad (1)$$

where, Y_i = TL intensity of sample i;

x_i = Applied dose to sample i;

a,b,c = Unknown parameters (coefficients);

ϵ_i = Error in sample i;

The errors, ϵ_is, are independent $N(0,\sigma_i^2)$ random variables.

1.2 POSSIBLE MODELS FOR ERRORS

1.2.1 POISSON DISTRIBUTION

A TL signal is actually a photon count. Therefore, normally it would be assumed that a Poisson distribution would be required. If the TL signal has a Poisson distribution, the variance of TL is the same as the expectation of the TL, E(TL). That is, the SD of a TL measurement is the square root of the mean, $\sqrt{E(TL)}$. Therefore, the percent error in TL is $[(1/\sqrt{E(TL)})*100\%]$; where, percent error = [(SD of TL)/(MEAN of TL)]*100%. For the saturating exponential model described in equation (1) the percent error in TL decreases with increasing applied dose due to the negative value of parameter 'b' if the signal is assumed to have a Poisson distribution. However, the actual observed error in the experimental data increases with increasing applied dose (e.g. Figure 0.3). This observed error is larger (see Chapter Five for numerical evidence on this point) probably owing to the subsample inhomogeneity. Therefore, the assumption that the TL has a Poisson distribution is inappropriate.

1.2.2 CONSTANT PERCENT ERROR

Straight-line least squares fits for young marine sediments were worked out by Berger et al. (1984) based on the assumptions listed on the following page:

[1] There is no measurement error in the applied dose.

[2] There is a constant percent error (unknown-in-advance) in each TL measurement throughout each set of samples.

That is , Berger et al. use the model

$$Y_i = (a+b*D_i)+\sigma*(a+b*D_i)*\epsilon_i \qquad \text{——— (2)}$$

where, D_i is the applied dose;

$\epsilon_i \sim N(0,1)$.

For the model (equation (2)) of Berger et al. the percent error in a TL measurement is

$$\frac{\sigma*(a+b*D_i)}{a+b*D_i} = \sigma$$

which is constant as a function of D (added dose). In other words, this percent error is independent of the applied dose, D.

Since the percent error in a TL measurement which has a Poisson distribution depends on the applied dose, a more realistic model is to consider a random number of grains, N, in each sample. The TL_N is a sum of all TL signals released from N sediment grains. If each of these N TL signals has a Poisson distribution with a parameter of λ, the mean and variance of the total TL (TL_N) can be written as on the following page (Bickel and Doksum, 1977):

$$E(TL_N) = \lambda * E(N)$$

$$Var(TL_N) = Var[E(TL_N|N)] + E[Var(TL_N|N)]$$

$$= \lambda^2 * Var(N) + \lambda * E(N).$$

The percent error in TL_N is as follows:

$$[\sqrt{\lambda^2 * Var(N) + \lambda * E(N)} \; / \; \lambda * E(N)] * 100\%$$

$$= [\sqrt{Var(N) + (E(N)/\lambda)} \; / \; E(N)] * 100\%.$$

For large λ the percent error in TL_N is approximately equal to $[\sqrt{Var(N)}/E(N)]$. This percent error is independent of λ. In other words, this percent error is a constant. Note that the Poisson distribution with large mean is quite normal in shape.

For the proposed non-linear saturating exponential model, the constant percent error means:

$$\frac{\sigma_i}{a+b*\exp(-cx_i)} = \sigma.$$

The Standard Deviation (SD) of a TL measurement, $\{\sigma * [a+b*\exp(-cx_i)]\}$, indicates that a weight, W_i which depends on the parameters 'a', 'b', 'c', is assigned to each TL measurement. Here, W_i is the inverse of the variance and has the form $[a+b*\exp(-cx_i)]^{-2}$. Therefore, another way of writing the model (equation (1)) is shown on the following page:

$$Y_i = a+b*\exp(-cx_i) + (\sigma/\sqrt{W_i})*\epsilon_i \qquad \text{——— (3)}$$

where, σ = constant = relative error;

W_i = weight = $[a+b*\exp(-cx_i)]^{-2} = g(x_i,\theta)$;

θ = parameters 'a', 'b', and 'c';

$\epsilon_i \sim N(0,1)$.

For the R-Γ procedure a non-linear saturating exponential model is used to fit the experimental data because of the expected saturation of electron traps contributing to the TL signal and the physical characteristics of the data. Therefore, a model with a saturating exponential mean and an unknown constant percent error are used for each curve. In the next Chapter, the estimation of the parameters (coefficients) of this model will be described and discussed.

CHAPTER 2

METHODS FOR ESTIMATING THE PARAMETERS OF THE MODEL

For this project the Iteratively Reweighted Least Squares (IRLS) method provided by the BMDP3R program from the BMDP (Biomedical Computer Programs, UCLA Press) Statistical Software manual is applied to estimate the parameters of the proposed saturating exponential model. In addition to this IRLS scheme, the theories of another two estimation schemes are described in this Chapter. These three methods, Non-linear Least Squares method, Maximum Likelihood method and Iteratively Reweighted Least Squares method will be illustrated in sections 2.1.1, 2.1.2 and 2.1.3, respectively. Finally, in section 2.2 the conclusion that these three estimation schemes are approximately the same is derived when σ is small.

2.1 DESCRIPTIONS OF METHODS OF ESTIMATION

2.1.1 NON-LINEAR LEAST SQUARES METHOD

In general, the polynomial and exponential models have the form

$$Y_i \sim N(f_i(a,b,c), \sigma^2 W_i^{-1}) \qquad \text{——— (4)}$$

$$\text{for } i = 1,2,3,\cdots,n.$$

For constant percent error the weight W_i depends on the parameters 'a', 'b', 'c', via $W_i = [1/f_i^2(a,b,c)]$ (Chapter One).

Therefore, the parameters of the saturating exponential model are estimated in this method (NLLS) by minimizing the equation of Residual Sum of Squares (RSS):

$$RSS = \sum_{i=1}^{n} [W_i(a,b,c)]*[Y_i - f_i(a,b,c)]^2 \qquad \text{——— (5).}$$

The estimates are obtained by setting

$$\partial RSS/\partial \hat{a} = 0$$

$$\partial RSS/\partial \hat{b} = 0$$

$$\partial RSS/\partial \hat{c} = 0.$$

Throughout this Chapter $\partial/\partial\hat{\theta}$ means differentiate with respect to θ and evaluate at $\hat{\theta}$.

2.1.2 MAXIMUM LIKELIHOOD METHOD

Assume that the dependent variable, Y_i, is normally distributed with a mean of $[a+b*\exp(-cx_i)]$ and a variance of $\{[a+b*\exp(-cx_i)]*\sigma\}^2$. For the model (equation (3)) the likelihood function for $Y_1, \ldots, Y_n$ is

$$L = g(Y_1)\cdot g(Y_2)\cdots g(Y_n).$$

In the case of the saturating exponential model this becomes

$$\{1/[(2\pi)^{n/2} \prod_{i=1}^{n} \sigma_i]\}*\exp\{-\sum_{i=1}^{n} [Y_i - (a+b*\exp(-cx_i))]^2/2\sigma_i^2\} \qquad \text{——— (6)}$$

$$\text{where, } \sigma_i = [a+b*\exp(-cx_i)]*\sigma.$$

The log likelihood function is shown on the following page:

$$\ln L = [(-n/2)*\ln(2\pi)] - \sum_{i=1}^{n}\{\ln[\sigma*(a+b*\exp(-cx_i))]\} - (1/2)*\sum_{i=1}^{n}\{[Y_i-(a+b*\exp(-cx_i))]^2/[\sigma*(a+b*\exp(-cx_i))]^2\} \quad \text{——— (7).}$$

The first derivatives of this log likelihood function with respect to parameters, 'a', 'b', 'c', and 'σ', are expressed as follows:

$$\partial \ln L/\partial a = \sum_{i=1}^{n}\{\frac{-1}{a+b*\exp(-cx_i)} + \frac{Y_i*[Y_i-a-b*\exp(-cx_i)]}{\sigma^2*[a+b*\exp(-cx_i)]^3}\}$$

$$\partial \ln L/\partial b = \sum_{i=1}^{n}\{\frac{-\exp(-cx_i)}{a+b*\exp(-cx_i)} + \frac{Y_i*\exp(-cx_i)*[Y_i-a-b*\exp(-cx_i)]}{\sigma^2*[a+b*\exp(-cx_i)]^3}\}$$

$$\partial \ln L/\partial c = \sum_{i=1}^{n}\{\frac{b*x_i*\exp(-cx_i)}{a+b*\exp(-cx_i)} + \frac{Y_i*b*x_i*\exp(-cx_i)*[Y_i-a-b*\exp(-cx_i)]}{\sigma^2*[a+b*\exp(-cx_i)]^3}\}$$

$$\partial \ln L/\partial \sigma = \sum_{i=1}^{n}\{\frac{-1}{\sigma} + \frac{1}{\sigma^3} * [\frac{Y_i-a-b*\exp(-cx_i)}{a+b*\exp(-cx_i)}]^2\}$$

——— (8).

The MLEs, $\hat{a}$, $\hat{b}$, $\hat{c}$, $\hat{\sigma}$, are then solved by setting the above equations to zero.

2.1.3 ITERATIVELY REWEIGHTED LEAST SQUARES

If the weight W_i did not depend on the parameters 'a', 'b' and 'c' then the MLEs of 'a', 'b' and 'c' would simply minimize RSS of equation (5). If the weight W_i does depend on the

parameters 'a', 'b' and 'c', two cases should be considered. These two cases are:

[A] $f_i(a,b,c)$ are linear in parameters 'a', 'b' and 'c'.

and

[B] $f_i(a,b,c)$ are non-linear in parameters 'a', 'b' and 'c'.

They are illustrated as follows:

[A] $f_i(a,b,c)$ are linear in parameters 'a', 'b' and 'c'.

When the function $f_i(a,b,c)$ is linear, the quantity RSS, can be minimized exactly by the technique of Weighted Least Squares (WLS). The technique of Iteratively Reweighted Least Squares (IRLS) proceeds as follows:

(i) With each W_i, set W_i to be one and carry out WLS to obtain the estimates, $\hat{a}_0$, $\hat{b}_0$, $\hat{c}_0$.

(ii) Replace the weight by $W_i(\hat{a}_0,\hat{b}_0,\hat{c}_0)$ then perform WLS to get another set of estimates, $\hat{a}_1$, $\hat{b}_1$ and $\hat{c}_1$.

(iii) Iterate step (ii) until the estimates do not change.

That is, calculate the weights using the updated estimates, $\hat{a}_k$, $\hat{b}_k$ and $\hat{c}_k$ to obtain $W_i(\hat{a}_k,\hat{b}_k,\hat{c}_k)$ then solve the following equations to obtain the new estimates, namely, $\hat{a}_{k+1}$, $\hat{b}_{k+1}$, $\hat{c}_{k+1}$:

$$\sum_{i=1}^{n}[W_i(\hat{a}_k,\hat{b}_k,\hat{c}_k)]*[Y_i-f_i(\hat{a}_{k+1},\hat{b}_{k+1},\hat{c}_{k+1})]*(\partial f_i/\partial a) = 0$$

$$\sum_{i=1}^{n}[W_i(\hat{a}_k,\hat{b}_k,\hat{c}_k)]*[Y_i-f_i(\hat{a}_{k+1},\hat{b}_{k+1},\hat{c}_{k+1})]*(\partial f_i/\partial b) = 0$$

$$\sum_{i=1}^{n}[W_i(\hat{a}_k,\hat{b}_k,\hat{c}_k)]*[Y_i-f_i(\hat{a}_{k+1},\hat{b}_{k+1},\hat{c}_{k+1})]*(\partial f_i/\partial c) = 0.$$

Note that the above equations are a linear system in $\hat{a}_{k+1}$, $\hat{b}_{k+1}$, $\hat{c}_{k+1}$ because $(\partial f_i/\partial a)$, $(\partial f_i/\partial b)$ and $(\partial f_i/\partial c)$ do not depend on 'a', 'b' and 'c'. The estimates are iteratively estimated in this manner until they do not change any more. That is, the iteration is terminated when the following condition is reached,

$$\hat{a}_{k+1} = \hat{a}_k$$
$$\hat{b}_{k+1} = \hat{b}_k$$
$$\hat{c}_{k+1} = \hat{c}_k.$$

The final estimates solve the following equations:

$$\sum_{i=1}^{n}[W_i(\hat{a},\hat{b},\hat{c})]*[Y_i-f_i(\hat{a},\hat{b},\hat{c})]*(\partial f_i/\partial a) = 0$$
$$\sum_{i=1}^{n}[W_i(\hat{a},\hat{b},\hat{c})]*[Y_i-f_i(\hat{a},\hat{b},\hat{c})]*(\partial f_i/\partial b) = 0 \quad \text{——— (9).}$$
$$\sum_{i=1}^{n}[W_i(\hat{a},\hat{b},\hat{c})]*[Y_i-f_i(\hat{a},\hat{b},\hat{c})]*(\partial f_i/\partial c) = 0$$

[B] $f_i(a,b,c)$ are non-linear in parameters 'a', 'b' and 'c'.

When the function f_i is non-linear, one cannot immediately minimize RSS; therefore, the Gauss-Newton algorithm is used to calculate $\hat{a}_{k+1}$, $\hat{b}_{k+1}$, $\hat{c}_{k+1}$ from $\hat{a}_k$, $\hat{b}_k$, $\hat{c}_k$. The estimates $\hat{a}_k$, $\hat{b}_k$, $\hat{c}_k$ will converge to the roots of equation (9).

The Gauss-Newton algorithm works as follows:

Gauss-Newton Algorithm:

An ordinary least squares method is applied to the linear terms of the non-linear regression model in order to estimate the parameters of these linear terms. The non-linear terms in the model are approximated by the linear terms of a Taylor series expansion. Equation (3) in Chapter One is a function of the applied dose and the parameters, $f(x_i,a,b,c)$. The linear terms in the Taylor series expansion of equation (3) at the initial parameter values can be written as follows:

$$\begin{aligned} f(x_i,a,b,c) \simeq\ & f(x_i,a^o,b^o,c^o) \\ & + (\partial f(x_i,a,b,c)/\partial a)_{a=a^o,b=b^o,c=c^o} * (a-a^o) \\ & + (\partial f(x_i,a,b,c)/\partial b)_{a=a^o,b=b^o,c=c^o} * (b-b^o) \\ & + (\partial f(x_i,a,b,c)/\partial c)_{a=a^o,b=b^o,c=c^o} * (c-c^o) \end{aligned} \quad \text{——— (10).}$$

It can be rewritten as

$$f(x_i,\Theta) \simeq f(x_i,\Theta^o) + \sum_{k=1}^{3} [\partial f(x_i,\Theta)/\partial \theta_k]_{\Theta=\Theta^o} * (\theta_k - \theta_k^o) \quad \text{——— (11)}$$

where,

Θ^o = a column vector of initial parameter values;

$$\Theta^o = \begin{bmatrix} \theta_1^o \\ \theta_2^o \\ \theta_3^o \end{bmatrix} = \begin{bmatrix} a^o \\ b^o \\ c^o \end{bmatrix};$$

$[\partial f(x_i,\Theta)/\partial \theta_k]_{\Theta=\Theta^o}$ = the partial derivative of equation (3) with respect to the kth parameter and is evaluated at all initial parameter values.

Our non-linear model, equation (3), has a form of

$$Y_i = f(x_i,\Theta)+\sigma * f(x_i,\Theta)*\epsilon_i \qquad \text{——— (12).}$$

Let $Y_i^\circ = Y_i - f(x_i,\theta^\circ)$; it follows from equations (11) and (12) that,

$$Y_i^\circ \simeq \{[\sum_{k=1}^{3} (\partial f(x_i,\Theta)/\partial\theta_k)]_{\Theta=\theta^\circ} * (\theta-\theta_k^\circ)\} + f(x_i,\Theta)*\sigma*\epsilon_i$$

——— (13).

Let

$$Y^\circ_{(n*1)} = \begin{bmatrix} Y_1 - f(x_1,\theta^\circ) \\ \vdots \\ Y_n - f(x_n,\theta^\circ) \end{bmatrix},$$

$P^\circ_{(nx3)}$ be the (nx3) matrix as follows:

$$\begin{bmatrix} (\partial f(x_1,\Theta)/\partial\theta_1)_{\Theta=\theta^\circ} & (\partial f(x_1,\Theta)/\partial\theta_2)_{\Theta=\theta^\circ} & (\partial f(x_1,\Theta)/\partial\theta_3)_{\Theta=\theta^\circ} \\ \cdot & & \\ \cdot & & \\ (\partial f(x_n,\Theta)/\partial\theta_1)_{\Theta=\theta^\circ} & (\partial f(x_n,\Theta)/\partial\theta_2)_{\Theta=\theta^\circ} & (\partial f(x_n,\Theta)/\partial\theta_3)_{\Theta=\theta^\circ} \end{bmatrix}$$

[NOTE]: the first column in $P^\circ_{(nx3)}$ is a column of 1's.

and,

$$\beta^\circ_{(3*1)} = \begin{bmatrix} \theta_1-\theta_1^\circ \\ \theta_2-\theta_2^\circ \\ \theta_3-\theta_3^\circ \end{bmatrix} = \begin{bmatrix} a-a^\circ \\ b-b^\circ \\ c-c^\circ \end{bmatrix} = \Theta-\theta^\circ \qquad \text{——— (14),}$$

then equation (13) can be written in matrix notation as

$$Y^0 \sim N(P^0\beta^0, \sigma^2 W^{-1})$$

where,

$$W = \begin{bmatrix} (a+b*\exp(-cx_1))^{-2} & & \\ & \ddots & \\ & & (a+b*\exp(-cx_n))^{-2} \end{bmatrix}.$$

This model can be rewritten as

$$Y^0 \simeq P^0\beta^0 + \epsilon^0 \qquad \text{——— (15)}$$

where, $\epsilon^0 \sim N(0, \sigma^2 W^{-1})$.

Let $g^0 = W^{0\frac{1}{2}}\epsilon$, then $E(g^0) = 0$, and

$$\text{Var}(g^0) = E(g^0 g^{0\prime}) = E[W^{0\frac{1}{2}}\epsilon(W^{0\frac{1}{2}}\epsilon)'] = W^{0\frac{1}{2}}E(\epsilon\epsilon')W^{0\frac{1}{2}}$$
$$= W^{0\frac{1}{2}} W^{0-\frac{1}{2}} W^{0-\frac{1}{2}} W^{0\frac{1}{2}}\sigma^2 = I\sigma^2.$$

Therefore, g^0 becomes as follows:

$$g^0 \sim N(0, I\sigma^2).$$

Multiplying equation (15) by $W^{0\frac{1}{2}}$,

$$W^{0\frac{1}{2}}Y^0 \simeq W^{0\frac{1}{2}} P^0\beta^0 + W^{0\frac{1}{2}}\epsilon^0$$

or $$Z^0 \simeq S^0\beta^0 + g^0 .$$

The estimates are obtained by the ordinary least squares method which is shown on the following page:

$$\hat{\beta}^0 = (S^{0'}S^0)^{-1}S^{0'}Z^0.$$

The estimates are then reexpressed in terms of the original variable Y^0 as

$$\hat{\beta}^0 = (P^{0'}W^{0'\frac{1}{2}}W^{0\frac{1}{2}}P^0)^{-1}(P^{0'}W^{0'\frac{1}{2}})(W^{0\frac{1}{2}}Y^0)$$

or $$\hat{\beta}^0 = (P^{0'}W^0P^0)^{-1}(P^{0'}W^0Y^0) \qquad \text{——— (16).}$$

By evaluating equation (16), the estimated parameters of the linear terms from the Taylor series expansion of the nonlinear model is obtained. Now $\hat{\beta}^0$ is an estimate of $(\theta-\theta^0)$ so the updated estimates for the nonlinear model are obtained as follows:

$$\theta = \theta^0+\hat{\beta}^0 \qquad \text{——— (17).}$$

The scheme of Gauss-Newton algorithm and IRLS is therefore summarized in the following steps:

(i) Evaluate the weight of equation (5) with the initial parameter values. The method for finding the initial estimates will be described in Chapter Four.

(ii) Input the initial parameter values to equation (16) to obtain the estimated parameters of the linear terms from the Taylor series expansion of the non-linear model. To obtain the updated (new) estimates of the non-linear model, equation (17) is evaluated.

(iii) Recalculate the weights then repeat step (ii). Continue the process until estimates are changed very little. Again the

final estimate solve equation (9).

Minimizing the RSS means setting the following equations to zero:

$$\partial RSS/\partial\hat{\theta} = -2\sum_{i=1}^{n}\{W_i(\hat{a},\hat{b},\hat{c})*[Y_i-f_i(\hat{a},\hat{b},\hat{c})]*[\partial f_i(\hat{a},\hat{b},\hat{c})/\partial\hat{\theta}]\}$$
$$+\sum_{i=1}^{n}\{[\partial W_i(\hat{a},\hat{b},\hat{c})/\partial\hat{\theta}]*[Y_i-f_i(\hat{a},\hat{b},\hat{c})]^2\} \quad \text{——— (18)}$$

where, $\hat{\theta}$ are $\hat{a}$, $\hat{b}$, $\hat{c}$.

But the IRLS algorithm only sets the first term of equation (18) to zero for the estimates, $\hat{a}$, $\hat{b}$ and $\hat{c}$. This means that the IRLS algorithm at each step need not reduce the value of RSS. This algorithm can be carried out using BMDP3R. This BMDP program can be used in two ways as follows:

(1) The parameters are estimated simply by following the Gauss-Newton algotithm.

With this method the estimates are the IRLS estimates. In order to use this method; two additional commands have to be included to the Regress section of the BMDP3R program used for method (2). These two additional commands are illustrated as follows:

(a) Specify the number of iterations.

(b) Set the permissible number of halvings (see method (2) below) to be zero.

(2) In addition to the first two steps of the Gauss-Newton algorithm and the IRLS scheme mentioned on the previous page, this method carries out the steps listed as follows:

(i) At the $(k+1)^{th}$ iteration, evaluate the following equation:

$$[\ RRS^{(k+1)} - RRS^{(k)}\ ] \qquad \text{——— (19)}$$

where, $RRS^{(k+1)}$ = Residual sum of squares of the (k+1)th iteration (updated);

$RRS^{(k)}$ = Residual sum of squares of the kth iteration (previous).

(ii) If the $RSS^{(k+1)}$ is larger than the $RSS^{(k)}$, then replace the increment size, $\hat{\beta}^{0}$, by $(\hat{\beta}^{0}/2)$ and recompute the RSS. This halving increment procedure is continued until the RSS decreases.

With method (1) the BMDP3R program displays the parameter estimates and their associated asymptotic correlation matrices and asymptotic standard deviations on the output (Chapter Four).

For this project the estimates are obtained by the IRLS method using the BMDP3R program (method (1)). In the next section (2.2), the IRLS estimates shown to be approximately equal to the MLEs when σ is small, will be discussed and derived.

2.2 DISCUSSION OF METHODS OF ESTIMATION

Up to this point three possible estimation schemes, Non-Linear Least Squares (NLLS), Maximum Likelihood (ML) and Iteratively Reweighted Least Squares (IRLS) are described in sections 2.1.1, 2.1.2 and 2.1.3, respectively. For this project the estimates are obtained by the IRLS algorithm using the BMDP3R program. Our discussion focuses on estimation of 'a', 'b' and 'c'. For all three methods σ is estimated via the last equation in (8). For the maximum likelihood estimates the four equations in (8) must be solved simultaneously since σ appears in each equation. The other two methods give a set of three estimating equations for 'a', 'b' and 'c' which may be solved without reference to σ. The following discussion will focus on the fact that the IRLS and the NLLS estimates are the same as the MLEs when σ is small.

2.2.1 MAXIMUM LIKELIHOOD ESTIMATION

Each observation, Y_i, has a normal distribution such as that mentioned in (4) on page one of this chapter, a more general form of the likelihood function can be written as follows:

$$L = \frac{1}{(2\pi)^{n/2} \prod_{i=1}^{n} (\sigma/\sqrt{W_i})} * \exp\{-[\sum_{i=1}^{n} (Y_i - f_i)^2]/[2*(\sigma^2/W_i)]\}$$

where, $f_i = f_i(a,b,c)$ = The proposed model is a function of parameters, 'a', 'b' and 'c';

$W_i = W_i(a,b,c)$ = The weight is a function of parameters, 'a', 'b' and 'c'.

The log likelihood function is

$$\ln L = (-n/2)*\ln(2\pi)+(1/2)*\sum_{i=1}^{n}(\ln W_i)-n\ln\sigma-\sum_{i=1}^{n}\{[(Y_i-f_i)^2*W_i]/2\sigma^2\}.$$

The maximum likelihood estimators are then obtained by solving the following equation:

$$U_{MLE}(\hat{\theta}) = \partial \ln L/\partial\hat{\theta} = (1/2)*\sum_{i=1}^{n}[(\partial W_i/\partial\hat{\theta})] - (1/\sigma^2)*\sum_{i=1}^{n}[W_i(Y_i-f_i)*(\partial f_i/\partial\hat{\theta})] - (1/2\sigma^2)*\sum_{i=1}^{n}[(Y_i-f_i)^2*(\partial W_i/\partial\hat{\theta})] = 0 \quad \text{——— (20).}$$

(The likelihood equation for σ may be solved explicitly to give $\hat{\sigma}^2 = [(1/n)*\sum_{i=1}^{n}W_i*(Y_i-f_i)^2]$.)

The mean vector and variance-covariance matrix for the first three components of $U_{MLE}(\theta)$ are:

$$E[U_{MLE}(\theta)] = (1/2)*E\{\sum_{i=1}^{n}[(\partial \ln W_i/\partial\theta)]\} - (1/\sigma^2)*E\{\sum_{i=1}^{n}[W_i*(Y_i-f_i)*(\partial f_i/\partial\theta)]\} - (1/2\sigma^2)*E\{\sum_{i=1}^{n}[(Y_i-f_i)^2*(\partial W_i/\partial\theta)]\} = (1/2)*\{[\sum_{i=1}^{n}[\partial W_i/\partial\theta)/W_i]\} - 0 - (1/2\sigma^2)*\sum_{i=1}^{n}[(\sigma^2/W_i)*(\partial W_i/\partial\theta)] = 0 \quad \text{——— (21)}$$

and, $\text{Var}\,[U_{MLE}(\theta)] = \text{Var}\,\{(1/2)*\sum_{i=1}^{n}[(\partial \ln W_i/\partial\theta)]\}$

$+ \text{Var}\,\{(1/\sigma^2)*\sum_{i=1}^{n}[W_i*(Y_i-f_i)*(\partial f_i/\partial\theta)]\}$

$+ \text{Var}\,\{(1/2\sigma^2)*\sum_{i=1}^{n}[(Y_i-f_i)^2*(\partial W_i/\partial\theta)]\}$

$= 0 + \sum_{i=1}^{n}\{(W_i^2/\sigma^4)*[(\partial f_i/\partial\theta)(\partial f_i/\partial\theta)^T]*(\sigma^2/W_i)\}$

$+ (1/4\sigma^4)*\sum_{i=1}^{n}\{[(\partial W_i/\partial\theta)(\partial W_i/\partial\theta)^T]*(2*\sigma^4/W_i^2)\}$

$= \sum_{i=1}^{n}\{(W_i/\sigma^2)*[(\partial f_i/\partial\theta)(\partial f_i/\partial\theta)^T]\}$

$+ (2/4)*\sum_{i=1}^{n}[(\partial \ln W_i/\partial\theta)(\partial \ln W_i/\partial\theta)^T]$

$= (1/\sigma^2)*\{\sum_{i=1}^{n} W_i*[(\partial f_i/\partial\theta)(\partial f_i/\partial\theta)^T]\}$

$+ (1/2)*\sum_{i=1}^{n}[(\partial \ln W_i/\partial\theta)(\partial \ln W_i/\partial\theta)^T]$ ——— (22).

When σ is small, the second term of equation (22) is very small compared to the first term. Therefore

$$\text{Var}\,[U_{MLE}(\theta)\,] \simeq (1/\sigma^2)*\sum_{i=1}^{n}\{\,W_i*[(\partial f_i/\partial\theta)(\partial f_i/\partial\theta)^T]\}$$

when σ is small.

[NOTE]: $\text{Var}\,(Y_i-f_i)^2 = \text{Var}\,\{(\sigma^2/W_i)[N(0,1)]^2\} = 2\sigma^4/W_i^2$.

$\text{Var}\,(Y_i-f_i) = E\,(Y_i-f_i)^2 = \sigma^2/W_i$.

$E\,(Y_i-f_i) = 0$.

$\{[(\partial W_i/\partial\theta)(\partial W_i/\partial\theta)^T]/W_i^2\} = (\partial \ln W_i/\partial\theta)(\partial \ln W_i/\partial\theta)^T$.

The covariance terms in $\text{Var}[U_{MLE}(\theta)]$, $\text{Var}[U_{IRLS}(\theta)]$ and $\text{Var}[U_{NLLS}(\theta)]$ are zero because $E(Y_i-f_i)^3 = 0$.

2.2.2 ITERATIVELY REWEIGHTED LEAST SQUARES

The IRLS algorithm was discussed in section 2.1.3. The IRLS estimates can be obtained by setting only the second term of equation (20) to zero (see equation (23)) which is the same as solving equation (5).

$$U_{IRLS}(\hat{\theta}) = -(1/\sigma^2)*\sum_{i=1}^{n}[W_i*(Y_i-f_i)*(\partial f_i/\partial\hat{\theta})] = 0 \quad \text{——— (23)}$$

The expectation and the variance of $U_{IRLS}(\theta)$ are shown as follows:

$$E\,[U_{IRLS}(\theta)] = E\,\{(-1/\sigma^2)*\sum_{i=1}^{n}[W_i*(Y_i-f_i)*(\partial f_i/\partial\theta)]\} = 0 \quad \text{——— (24);}$$

$$\begin{aligned} Var\,[U_{IRLS}(\theta)] &= Var\,\{(-1/\sigma^2)*\sum_{i=1}^{n}[W_i*(Y_i-f_i)*(\partial f_i/\partial\theta)]\} \\ &= (1/\sigma^4)*\sum_{i=1}^{n}\{W_i^2*[(\partial f_i/\partial\theta)(\partial f_i/\partial\theta)^T]*(\sigma^2/W_i)\} \\ &= (1/\sigma^2)*\sum_{i=1}^{n}\{W_i*[(\partial f_i/\partial\theta)(\partial f_i/\partial\theta)^T]\} \end{aligned} \quad \text{——— (25).}$$

2.2.3 NON-LINEAR LEAST SQUARES

Solving equation (18) for the NLLS estimates is the same as setting the second and the third terms of equation (20) to zero; that is:

$$\begin{aligned} U_{NLLS}(\hat{\theta}) = &-(1/\sigma^2)*\sum_{i=1}^{n}[W_i*(Y_i-f_i)*(\partial f_i/\partial\hat{\theta})] \\ &-(1/2\sigma^2)*\sum_{i=1}^{n}[(Y_i-f_i)^2*(\partial W_i/\partial\hat{\theta})] = 0 \end{aligned} \quad \text{——— (26).}$$

The expection of $U_{NLLS}(\theta)$ is not zero. It is shown as follows:

$$
\begin{aligned}
E[U_{NLLS}(\theta)] &= E\{-(1/\sigma^2)*\sum_{i=1}^{n}[W_i*(Y_i-f_i)*(\partial f_i/\partial\theta)]\} \\
&\quad + E\{(-1/2\sigma^2)*\sum_{i=1}^{n}[(Y_i-f_i)^2*(\partial W_i/\partial\theta)]\} \\
&= (-1/2\sigma^2)*\sum_{i=1}^{n}[(\sigma^2/W_i)*(\partial W_i/\partial\theta)] \\
&= (-1/2)*\sum_{i=1}^{n}(\partial \ln W_i/\partial\theta) \qquad \text{——— (27).}
\end{aligned}
$$

The variance of $U_{NLLS}(\theta)$ is shown as follows:

$$
\begin{aligned}
\text{Var}[U_{NLLS}(\theta)] &= \text{Var}\{(1/\sigma^2)*\sum_{i=1}^{n}[W_i(Y_i-f_i)*(\partial f_i/\partial\theta)]\} \\
&\quad + \text{Var}\{(1/2\sigma^2)*\sum_{i=1}^{n}[(Y_i-f_i)^2*(\partial f_i/\partial\theta)]\} \\
&= \sum_{i=1}^{n}\{(W_i^2/\sigma^4)*[(\partial f_i/\partial\theta)(\partial f_i/\partial\theta)^T]*(\sigma^2/W_i)\} \\
&\quad + (1/4\sigma^4)*\sum_{i=1}^{n}\{[(\partial W_i/\partial\theta)(\partial W_i/\partial\theta)^T]*(2*\sigma^4/W_i^2)\} \\
&= \sum_{i=1}^{n}\{(W_i/\sigma^2)[*(\partial f_i/\partial\theta)(\partial f_i/\partial\theta)^T]\} \\
&\quad + (2/4)*\sum_{i=1}^{n}\{[(\partial W_i/\partial\theta)(\partial W_i/\partial\theta)^T]/W_i^2\} \\
&= \sum_{i=1}^{n}\{(W_i/\sigma^2)[*(\partial f_i/\partial\theta)(\partial f_i/\partial\theta)^T]\} \\
&\quad + (2/4)*\sum_{i=1}^{n}[(\partial \ln W_i/\partial\theta)(\partial \ln W_i/\partial\theta)^T] \\
&= (1/\sigma^2)*\sum_{i=1}^{n}\{W_i*[(\partial f_i/\partial\theta)(\partial f_i/\partial\theta)^T]\} \\
&\quad + (2/4)*\sum_{i=1}^{n}[(\partial \ln W_i/\partial\theta)(\partial \ln W_i/\partial\theta)^T] \\
&= (2\sigma^2+1)\ \text{Var}[U_{IRLS}(\theta)] \\
&= \text{Var}[U_{MLE}(\theta)] \\
&\qquad \text{——— (28).}
\end{aligned}
$$

When σ is small, the second term of equation (28) is very small. Therefore, the variance of $U_{NLLS}(\theta)$ (equation (26)) is approximately:

$$
\text{Var}[U_{NLLS}(\theta)\ ] \approx (1/\sigma^2)*\sum_{i=1}^{n}\{W_i*[(\partial f_i/\partial\theta)(\partial f_i/\partial\theta)^T]\}
$$

when σ is small. The above information can be summarized in the following table: (NOTE: $M_i=[(\partial f_i/\partial\hat{\theta})(\partial f_i/\partial\hat{\theta})^T]$)

ESTIMATES	E[U(θ)]	Var[U(θ)]
MLE	0	$(1/\sigma^2) * \sum_{i=1}^{n}[W_i*M_i] * (2\sigma^2+1)$
IRLS	0	$(1/\sigma^2) * \sum_{i=1}^{n}[W_i*M_i]$
NLLS	$(-1/2)\sum_{i=1}^{n}(\partial \ln W_i/\partial\theta)$	$(1/\sigma^2) * \sum_{i=1}^{n}[W_i*M_i] * (2\sigma^2+1)$

2.2.4 DISCUSSION

If estimating equations have the form

$$U(\hat{\theta}) = 0 \qquad (29)$$

and have the properties

$$E[U(\theta)] = 0$$
$$Var[U(\theta)] = \Sigma,$$

then by Taylor expansion, equation (29) can be expressed as follows:

$$U(\hat{\theta}) = 0 = U(\theta)+(\hat{\theta}-\theta)*(\partial U/\partial\theta)+ \text{negligible terms.}$$

Ignoring the negligible terms in the above equation then it can be expressed on the following page:

$$(\hat{\theta}-\theta) \simeq -(\partial U/\partial\theta)^{-1} * U(\theta) \qquad \text{——— (30).}$$

If $U(\theta) \simeq N(0,\Sigma)$, then

$$(\hat{\theta}-\theta) \sim N(0, V^{-1}\Sigma V^{-1}) \qquad \text{——— (31)}$$

where, $V = -E(\partial U/\partial\theta)$.

For MLEs, the matrices Σ and V are equal to the Fisher Information Matrix, I. (Fisher Information Matrix is shown on the following page.) The variance term of (31) is then

$$V^{-1}\Sigma V^{-1} = I^{-1} I\ I^{-1} = I^{-1}.$$

Therefore, for MLEs the distribution of $(\hat{\theta}-\theta)$ has a form of

$$(\hat{\theta}-\theta) \sim N(0, I^{-1}).$$

By deriving the second derivatives of the log likelihood function (equation (31)) with respect to parameters, 'a', 'b', 'c', and 'σ', a symmetric (4x4) Fisher information matrix, I, is constructed as follows:

$$\begin{bmatrix} E(-\partial^2 lnL/\partial a^2) & E(-\partial^2 lnL/\partial a\partial b) & E(-\partial^2 lnL/\partial a\partial c) & E(-\partial^2 lnL/\partial a\partial\sigma) \\ & E(-\partial^2 lnL/\partial b^2) & E(-\partial^2 lnL/\partial b\partial c) & E(-\partial^2 lnL/\partial b\partial\sigma) \\ & & E(-\partial^2 lnL/\partial c^2) & E(-\partial^2 lnL/\partial c\partial\sigma) \\ & & & E(-\partial^2 lnL/\partial\sigma^2) \end{bmatrix}.$$

where,

E = Expectation and the values of 'a', 'b', 'c' and σ are the true parameter values.

The entries of the Fisher information matrix are shown as follows:

$$E(-\partial^2 \ln L/\partial a^2) = \sum_{i=1}^{n} \{(2\sigma^2+1)/[\sigma^2*(a+b*\exp(-cx_i))^2]\}$$

$$E(-\partial^2 \ln L/\partial a \partial b) = \sum_{i=1}^{n} \{[(2\sigma^2+1)*\exp(-cx_i)]/[\sigma^2*(a+b*\exp(-cx_i))^2]\}$$

$$E(-\partial^2 \ln L/\partial a \partial c) = \sum_{i=1}^{n} \{[-x_i*b*(2\sigma^2+1)*\exp(-cx_i)]/[\sigma^2*(a+b*\exp(-cx_i))^2]\}$$

$$E(-\partial^2 \ln L/\partial a \partial \sigma) = \sum_{i=1}^{n} \{2/[\sigma*(a+b*\exp(-cx_i))]\}$$

$$E(-\partial^2 \ln L/\partial b^2) = \sum_{i=1}^{n} \{[(2\sigma^2+1)*\exp(-2cx_i)]/[\sigma^2*(a+b*\exp(-cx_i))^2]\}$$

$$E(-\partial^2 \ln L/\partial b \partial c) = -\sum_{i=1}^{n} \{[b*x_i*(2\sigma^2+1)*\exp(-2cx_i)]/[\sigma^2*(a+b*\exp(-cx_i))^2]\}$$

$$E(-\partial^2 \ln L/\partial b \partial \sigma) = \sum_{i=1}^{n} \{[2*\exp(-cx_i)]/[\sigma*(a+b*\exp(-cx_i))]\}$$

$$E(-\partial^2 \ln L/\partial c^2) = \sum_{i=1}^{n} \{[b^2*x_i^2*(2\sigma^2+1)*\exp(-2cx_i)]/[\sigma^2*(a+b*\exp(-cx_i))^2]\}$$

$$E(-\partial^2 \ln L/\partial c \partial \sigma) = \sum_{i=1}^{n} \{[-2*b*x_i*\exp(-cx_i)]/[\sigma*(a+b*\exp(-cx_i))]\}$$

$$E(-\partial^2 \ln L/\partial \sigma^2) = \sum_{i=1}^{n} (2/\sigma^2).$$

The theoretical Variance-Covariance matrix is therefore obtained

by inverting the above Fisher information matrix.

When σ is small, the (3x3) upper left array of the (4x4) Fisher information matrix can be inverted to a (3x3) theoretical variance-covariance matrix that has nearly the same entries as those obtained by inverting the whole (4x4) Fisher information matrix. This may be seen as follows:

[1] The (3x3) upper left array of the (4x4) Fisher information matrix is proportional to $(1/\sigma^2)$;

[2] The remaining off-diagonal portions of this (4x4) Fisher information matrix, $E(-\partial^2 \ln L/\partial\theta\partial\sigma)$, (where, θ is 'a', 'b' or 'c') have the form as follows:

$$-\{(1/\sigma)*\sum_{i=1}^{n}[(\partial \ln W_i/\partial\theta)]\};$$

[3] The remaining diagonal portion, $E(-\partial^2 \ln L/\partial\sigma^2)$, is $(2n/\sigma^2)$ which is proportional to $(1/\sigma^2)$;

[4] The matrix $\sigma^2 I$ is therefore a block diagonal matrix plus a matrix proportional to σ. The matrix I^{-1} is then nearly the inverse of the block diagonal matrix so that $\hat{\sigma}$ and $\hat{a}$, $\hat{b}$, $\hat{c}$ are nearly uncorrelated.

From the table on page 32 we see that the Var $[U_{MLE}(\theta)]$ = Var $[U_{NLLS}(\theta)]$ ≃ Var $[U_{IRLS}(\theta)]$ for small σ. Moreover, for IRLS the matrix $V = E\ (\partial U/\partial\theta) = \text{Var}\ [U_{IRLS}(\theta)]$ and for NLLS $V = \text{Var}[U_{MLS}(\theta)]$. Thus all three methods lead to approximately the same value of $V^{-1}\Sigma V$.

Finally, for the NLLS estimates the following information is concluded from the results of equation (27) and (28) when σ is small:

$$E\ (\hat{\theta}-\theta) \simeq -V^{-1}[-\sum_{i=1}^{n}(\partial \ln W_i/\partial\theta)] \propto \sigma^2$$

and $$Var\ (\hat{\theta}-\theta) \simeq V^{-1}\ Var\ (U)\ V^{-1} \simeq \sigma^2 \qquad \text{——— (32)}$$

where, $V = -E(\partial U/\partial\theta) \propto (1/\sigma^2)$ (equation (28)).

$E(\hat{\theta}-\theta)$ is proportional to σ^2 which is small compared to the SE of $\hat{\theta}$. (The SE is proportional to σ.)

It should be noted that the IRLS and NLLS methods separate the estimates of σ from the estimation of the other parameters. The ML method requires the simultaneous solution of four equations; the other two methods give three equations not including σ and a simple formula for $\hat{\sigma}$.

2.3 SUMMARY

The general theory of estimating equations provide the roots of $U_{MLE}(\hat{\theta})$, $U_{IRLS}(\hat{\theta})$ and $U_{NLLS}(\hat{\theta})$ with asymptotic properties. All three methods produce variances of matrix form $\mathbf{M}^{-1}$ where

$$\mathbf{M} = \mathbf{I} + \mathbf{R}.$$

The entries in matrix I are proportional to $(1/\sigma^2)$ and those in matrix R are proportional to $(1/\sigma)$. For small σ, matrix R is negligible. The estimating functions, $U_{MLE}(\theta)$ and $U_{IRLS}(\theta)$, have mean values of zero but $U_{NLLS}(\theta)$ has a mean which is

proportional to σ^2 (equation (32)). The mean of $U_{NLLS}(\theta)$ is negligible because the SEs of the estimates are proportional to σ. The IRLS and the NLLS estimating schemes therefore lead to approximately the same answers as the ML estimating scheme when σ is small. For this project the IRLS algorithm is applied to calculate the estimates but the MLE theory is used to obtain the variance-covariance of the IRLS estimates because these are relatively simple to calculate. This technique will be justified by Monte Carlo studies of Chapter Four.

CHAPTER 3

ESTIMATIONS OF THE INTERSECTION POINTS AND THEIR ASSOCIATED VARIANCES

For the R-Γ procedure in dating sediments, accurate extrapolation is necessary to obtain the intersection point beyond the origin. In section 3.1 of this Chapter the method of accurately extrapolating the intersection points will be illustrated. It is followed in section 3.2 by the estimation of the variances of these intersection points by the maximum likelihood method.

3.1 ESTIMATION OF THE INTERSECTION POINTS

The intersection point is the point at which the TL intensities of both curves are the same. Referring to Figure 0.3 (Introduction) with 1A as the top curve, 1B the middle curve, and 1C the bottom curve, curves 1A and 1B can be described by the following equations:

$$\text{curve 1A:}\quad \hat{Y} = \hat{a}+\hat{b}*\exp(-\hat{c}\hat{x}^*) \qquad \text{——— (33)}$$

$$\text{curve 1B:}\quad \tilde{Y} = \tilde{a}+\tilde{b}*\exp(-\tilde{c}\hat{x}^*) \qquad \text{——— (34)}$$

where, $\hat{a}$, $\hat{b}$, $\hat{c}$ are estimated parameters of curve 1A;

$\tilde{a}$, $\tilde{b}$, $\tilde{c}$ are estimated parameters of curve 1B.

These estimated parameters are the IRLS estimates. They are obtained by fitting each data set to the saturating exponential

model separately with the IRLS algorithm using the BMDP3R program.

The estimated intersection point of curve 1A and curve 1B $(\hat{x}^*, \hat{Y}^*)$, is the point at which $\hat{Y} = \tilde{Y} = \hat{Y}^*$. It is shown as follows:

$$\hat{a}+\hat{b}*\exp(-\hat{c}\hat{x}^*) = \tilde{a}+\tilde{b}*\exp(-\tilde{c}\hat{x}^*) \qquad \text{——— (35)}$$

where, $\hat{x}^*$, the estimated intersection point, is a function of all six estimated parameters $\hat{a}$, $\hat{b}$, $\hat{c}$, $\tilde{a}$, $\tilde{b}$, $\tilde{c}$; that is, $\hat{x}^* = f(\hat{a}, \hat{b}, \hat{c}, \tilde{a}, \tilde{b}, \tilde{c})$.

In order to solve for $\hat{x}^*$, an IMSL routine called ZBRENT, a combination of linear interpolation, inverse quadratic interpolation, and a bisection algorithm procedure is applied to find the root of the following equation:

$$\hat{a}+\hat{b}*\exp(-\hat{c}\hat{x}^*)-(\tilde{a}+\tilde{b}*\exp(-\tilde{c}\hat{x}^*)) = 0 \qquad \text{——— (36).}$$

3.2 ESTIMATION OF VARIANCE OF THE INTERSECTION POINT

For $\hat{x}^*$ being a function of $\hat{a}$, $\hat{b}$, $\hat{c}$, $\tilde{a}$, $\tilde{b}$ and $\tilde{c}$ and x^* being a function of 'a_A', 'b_A', 'c_A', 'a_B', 'b_B', 'c_B', $(\hat{x}^*-x^*)$ can be approximated by Taylor expansion on the following page:

$$(\hat{x}^*-x^*) = f(\hat{a},\hat{b},\hat{c},\tilde{a},\tilde{b},\tilde{c})-f(a_A,b_A,c_A,a_B,b_B,c_B)$$
$$\simeq (\hat{a}-a_A)*(\partial f/\partial a_A)+(\hat{b}-b_A)*(\partial f/\partial b_A)+(\hat{c}-c_A)*(\partial f/\partial c_A)$$
$$+(\tilde{a}-a_B)*(\partial f/\partial a_B)+(\tilde{b}-b_B)*(\partial f/\partial b_B)+(\tilde{c}-c_B)*(\partial f/\partial c_B).$$

The expectation of this approximation is as follows:

$$E(\hat{x}^*-x^*) \simeq 0.$$

Its variance has the following form:

$$\begin{aligned}\mathrm{Var}(\hat{x}^*-x^*) \simeq\ & (\partial f/\partial a_A)^2*\mathrm{Var}(\hat{a})+(\partial f/\partial b_A)^2*\mathrm{Var}(\hat{b})+(\partial f/\partial c_A)^2*\mathrm{Var}(\hat{c})\\ & +2(\partial f/\partial a_A)*(\partial f/\partial b_A)*\mathrm{Cov}(\hat{a},\hat{b})+2(\partial f/\partial a_A)*(\partial f/\partial c_A)*\mathrm{Cov}(\hat{a},\hat{c})\\ & +2(\partial f/\partial b_A)*(\partial f/\partial c_A)*\mathrm{Cov}(\hat{b},\hat{c})\\ & +(\partial f/\partial a_B)^2*\mathrm{Var}(\tilde{a})+(\partial f/\partial b_B)^2*\mathrm{Var}(\tilde{b})+(\partial f/\partial c_B)^2*\mathrm{Var}(\tilde{c})\\ & +2(\partial f/\partial a_B)*(\partial f/\partial b_B)*\mathrm{Cov}(\tilde{a},\tilde{b})+2(\partial f/\partial a_B)*(\partial f/\partial c_B)*\mathrm{Cov}(\tilde{a},\tilde{c})\\ & +2(\partial f/\partial b_B)*(\partial f/\partial c_B)*\mathrm{Cov}(\tilde{b},\tilde{c})\\ =\ & (\nabla f)^T I'(\nabla f).\end{aligned}$$

Therefore, the estimated intersection point has approximately a normal distribution with a mean of x^* and an estimated variance $\mathrm{Var}(\hat{x}^*)$. With the IRLS estimates and their corresponding variance-covariance matrices calculated by the MLE theory the estimated variance of the intersection point can be obtained by using the equation (Serfling 1980) as follows:

$$\mathrm{Var}(f) \simeq (\nabla f)^T\ I'(\nabla f) \qquad \text{——— (37)}$$

where,

$f = f(\hat{a},\ \hat{b}\ ,\ \hat{c}\ ,\ \tilde{a},\ \tilde{b}\ ,\ \tilde{c}) = \hat{x}^*$;

$(\nabla f)^T$ = The transpose of the gradient array;
$= (\partial f/\partial\hat{a},\ \partial f/\partial\hat{b},\ \partial f/\partial\hat{c},\ -\partial f/\partial\tilde{a},\ -\partial f/\partial\tilde{b},\ -\partial f/\partial\tilde{c})$;

and

I' = Varianee-Covariance matrix of $(\hat{a},\hat{b},\hat{c},\tilde{a},\tilde{b},\tilde{c})$.

Each element in $(\nabla f)^T$ is obtained by evaluating the first derivatives of equation (35) with respect to each of the six estimated parameters. They are explicitly shown as follows:

$$\partial\hat{x}^*/\partial\hat{a} = \frac{1}{\hat{b}\hat{c}\exp(-\hat{c}\hat{x}^*)-\hat{b}\tilde{c}\exp(-\tilde{c}\hat{x}^*)}$$

$$\partial\hat{x}^*/\partial\hat{b} = \frac{\exp(-\hat{c}\hat{x}^*)}{\hat{b}\hat{c}\exp(-\hat{c}\hat{x}^*)-\hat{b}\tilde{c}\exp(-\tilde{c}\hat{x}^*)}$$

$$\partial\hat{x}^*/\partial\hat{c} = \frac{-\hat{b}\hat{x}^*\exp(-\hat{c}\hat{x}^*)}{\hat{b}\hat{c}\exp(-\hat{c}\hat{x}^*)-\hat{b}\tilde{c}\exp(-\tilde{c}\hat{x}^*)}$$

$$\partial\hat{x}^*/\partial\tilde{a} = \frac{1}{\hat{b}\tilde{c}\exp(-\tilde{c}\hat{x}^*)-\hat{b}\hat{c}\exp(-\hat{c}\hat{x}^*)}$$

$$\partial\hat{x}^*/\partial\tilde{b} = \frac{\exp(-\tilde{c}\hat{x}^*)}{\hat{b}\tilde{c}\exp(-\tilde{c}\hat{x}^*)-\hat{b}\hat{c}\exp(-\hat{c}\hat{x}^*)}$$

$$\partial\hat{x}^*/\partial\tilde{c} = \frac{-\tilde{b}\hat{x}^*\exp(-\tilde{c}\hat{x}^*)}{\hat{b}\tilde{c}\exp(-\tilde{c}\hat{x}^*)-\hat{b}\hat{c}\exp(-\hat{c}\hat{x}^*)}.$$

Because data 1A are independent of data 1B, the covariances of 1A and 1B are zero. Therefore, the theoretical Variance-Covariance matrix, I', can be written as follows:

$$\begin{bmatrix} {}_{A}I'_{3X3} & 0_{3X3} \\ 0_{3X3} & {}_{B}I'_{3X3} \end{bmatrix}$$

where, ${}_{A}I'_{3X3}$ = The (3X3) upper left array of the (4X4) theoretical variance-covariance matrix for data set 1A;

${}_{B}I'_{3X3}$ = The (3X3) upper left array of the (4X4) theoretical variance-covariance matrix

for data set 1B;
0_{3X3} = (3X3) zero matrix with all entries of zero.

The SDs (uncertainties) of these intersection points are obtained by $\sqrt{Var(f)}$.

If the estimated intersection point has approximately a normal distribution, interval estimates can be calculated. Interval estimates for the estimated intersection point (a margin of uncertainty) can be calculated by constructing confidence intervals for the intersection point. For the small sample sizes studied in this paper (n=11 to n=17) the confidence intervals of the intersection point are calculated by the following equation:

$$\hat{x}^* \pm \sqrt{Var(f)} \cdot t_{n_A+n_B-6} \qquad \text{——— (38).}$$

Here, a t-distribution critical point with a degrees of freedom of (n_A+n_B-6) is used because the variance of this estimated intersection point is an estimated value using equation (37). Proceeding by analogy with the regression situation it is hoped that the distribution of

$$\frac{\hat{x}^*-x^*}{\sqrt{Var(f)}} \qquad \text{——— (39)}$$

will be well approximated by a t-distribution with (n_A+n_B-6) degrees of freedom.

CHAPTER 4

MONTE CARLO SIMULATION

For the non-linear saturating exponential model, $f_i(a,b,c)$, having a weight as a function of parameters 'a', 'b' and 'c', initial parameters are required to invoke an IRLS algorithm using the BMDP3R program (Chapter Two). Two possible methods of obtaining the initial parameters described in section 4.1 are the Graphical Method and the Quadratic Equation Method. In section 4.2 Monte Carlo study is applied to examine the quality of the estimation scheme discussed in Chapter Two.

4.1 HOW TO OBTAIN INITIAL ESTIMATES

In order to proceed with the IRLS algorithm using the BMDP3R program, initial estimates (coefficients) of the non-linear saturating exponential model are required (section 2.1.3; Chapter Two). Two possible methods of obtaining these are the Graphical Method and the Quadratic equations as described in sections 4.1.1 and 4.1.2, respectively.

4.1.1 GRAPHICAL METHOD

The non-linear saturating exponential model has the following form:

$$f(D) = E(TL) = a+b*\exp(-c*D) \qquad \text{——— (40).}$$

where, D = applied dose;

a,b,c = coefficients (parameters).

When increasing the applied dose the second term in equation (40), [b*exp(-c*D)], tends toward zero. Thus for large applied doses, D, the TL measurements approaching a constant 'a'. Therefore, plotting TL intensities versus their corresponding applied doses produces a curve of positive slope followed by a plateau at higher dose levels. The value of 'a' is the thermoluminescence intensity found by extrapolating the plateau back to the TL intensity axis. The plot is shown on Figure 4.1.1 of the following page:

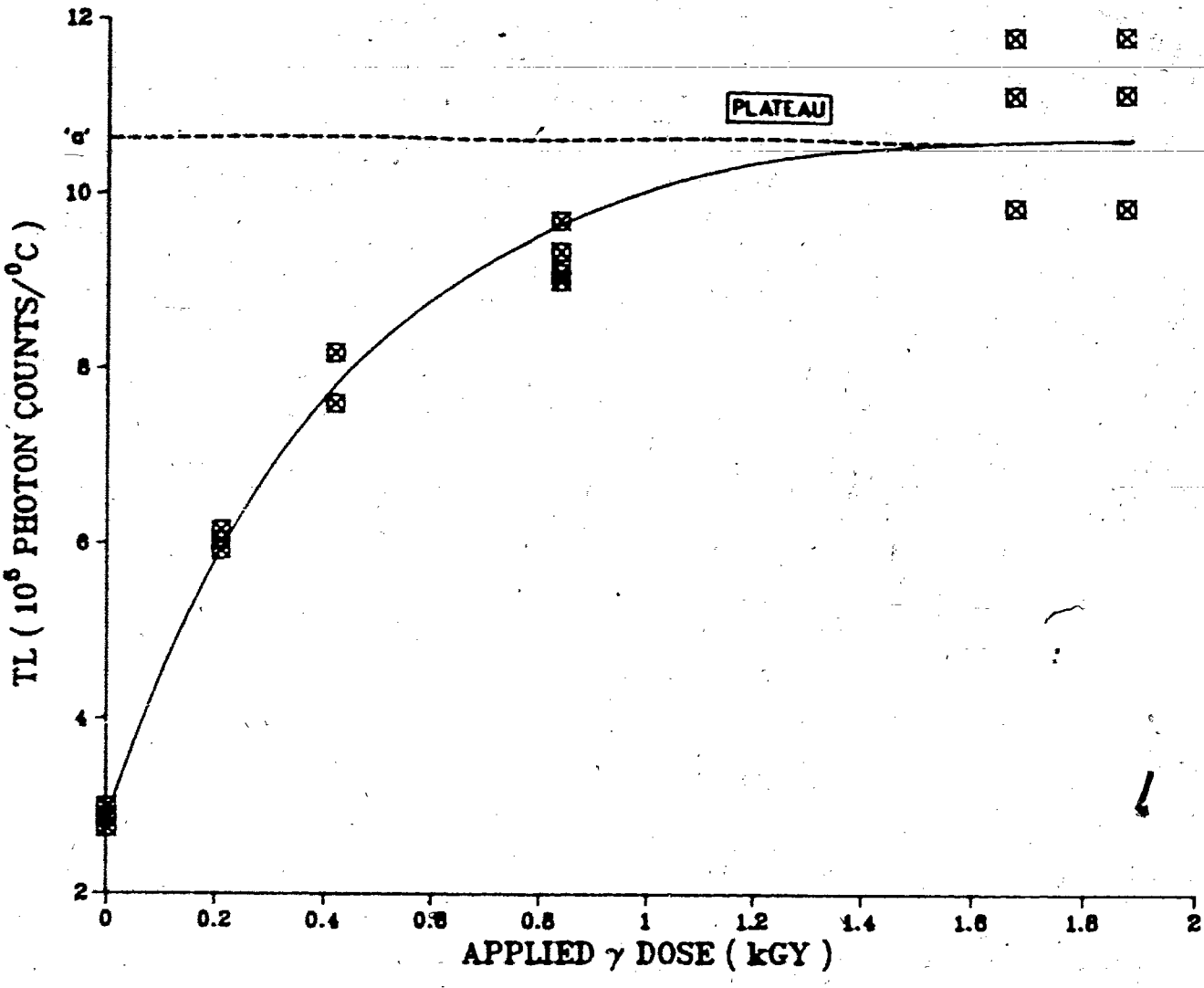

[Figure 4.1.1] Thermoluminescence versus applied dose to obtain the initial parameter 'a', for the Graphical Method.
A plateau is reacheo at some high applied dose levels. The value of parameter 'a' in equation (40) is the thermoluminescence intensity by extrapolating this plateau back to the TL axis.

Having found 'a', the initial values of 'b' and 'c' are obtained algebraiclly a few steps after expressing equation (40) as follows :

$$(TL-a) = b*\exp(-c*D) \qquad \text{——— (41).}$$

Here parameter 'b' has a negative value because experimentally the TL measurements tend to increase with increasing applied dose (D). Taking the logarithm on both sides of equation (41),

$$\ln(a-TL) = \ln(-b)-c*D \qquad \text{——— (42)}$$

produces a straight line with a slope of (-c) and an intercept of (ln(-b)). If plotting [ln(a-TL)] versus D, the parameter values of 'b' and 'c' will be obtained algebraically by equating the intercept to (ln(-b)) and the slope to (-c). Of course values of TL larger than 'a' must be omitted. In Figure 4.1.1 all data points with applied dose of 1.6 or more would be omitted.

4.1.2 QUADRATIC EQUATION METHOD

The Quadratic Equation Method proceeds by the following three steps:

(i) Empirically at each applied dose level a number of TL intensities are recorded from several AL discs (introduction). For the quadratic equation method the average of these TL intensities at each applied dose level is required. A quadratic equation is then sought to fit the data set, in which the average TL intensity is calculated at each applied dose level. The above description is illustrated on Figure 4.1.2 of the following page:

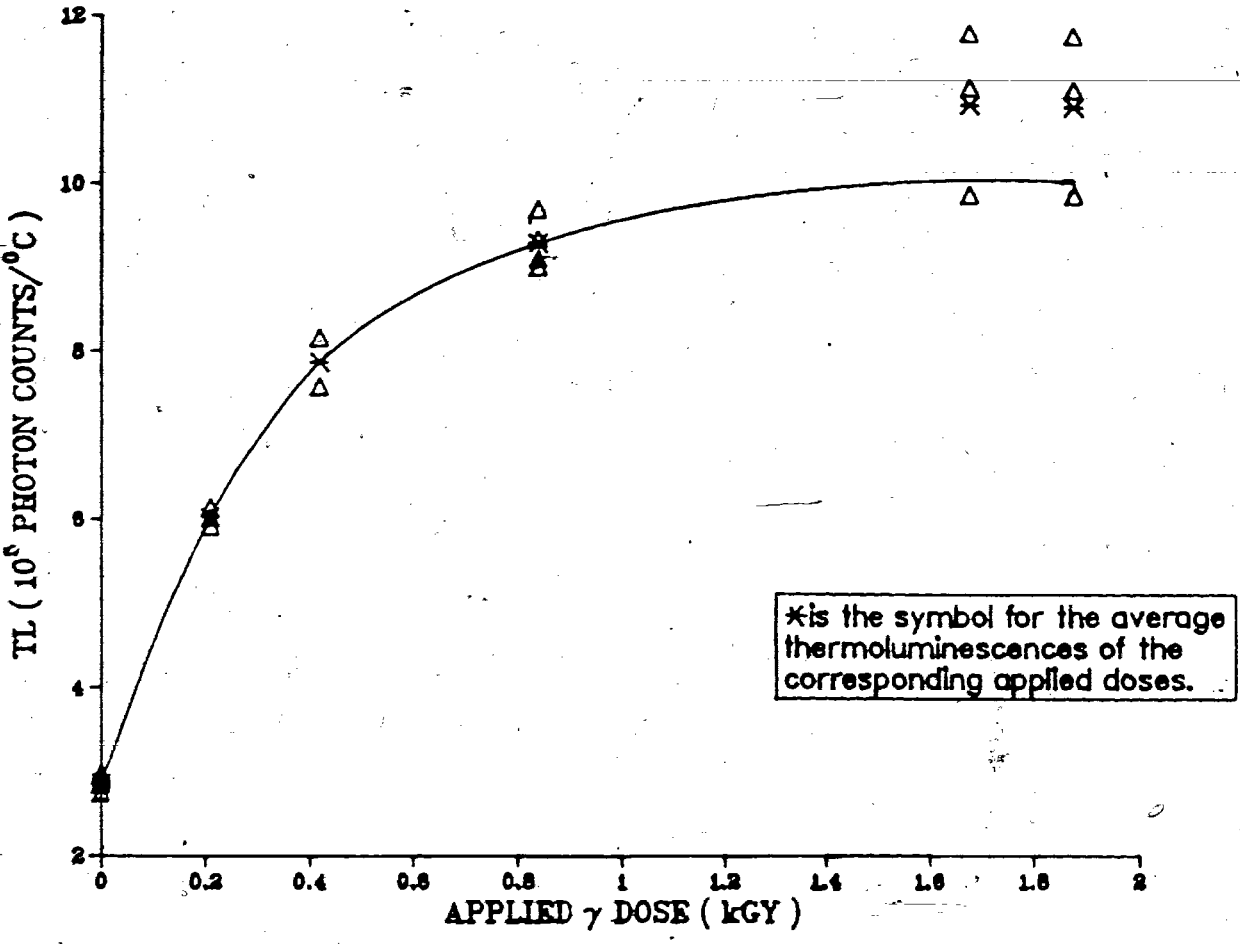

[Figure 4.1.2] Thermoluminescence versus applied dose to obtain the initial parameters for the Quadratic Equation Method.
$\overline{TL}_0$, $\overline{TL}_1$, $\overline{TL}_2$, $\overline{TL}_3$, $\overline{TL}_4$ and $\overline{TL}_5$ are the average thermoluminescences for the given doses D_0, D_1, D_2, D_3, D_4, D_5, respectively.

The quadratic equation has a form of

$$r_1+r_2*D+r_3*D^2 = \overline{TL}_D \qquad \text{——— (43)}$$

where, r_1, r_2, r_3 = The coefficients; constants;

D = Applied dose;

$\overline{TL}_D$ = Average TL intensity at the applied dose, D.

This quadratic equation approximates the saturating exponential curve for the same data set. (To get r_1, r_2 and r_3 simply regress $\overline{TL}_D$ on D, D^2.)

(ii) The first and the second derivatives of the quadratic equation (equation (43)) and the saturating exponential equation (equation (40)) are derived separately. This is followed by the evaluation of these and their corresponding first and second derivatives at dose zero (i.e. D=0). It can be summarized as follows:

Quadratic Equation: (r_1, r_2, r_3 are known coefficients)

$$r_1+r_2*D+r_3*D^2 = \overline{TL}_D; \quad r_1 = \overline{TL}_{D=0} \qquad \text{——— (44)}$$

[First Derivative]:

$$r_2+2*r_3*D = \overline{TL}_D'; \quad r_2 = \overline{TL}_{D=0}' \qquad \text{——— (45)}$$

[Second Derivative]:

$$2*r_3 = \overline{TL}_D''; \quad 2r_3 = \overline{TL}_{D=0}'' \qquad \text{——— (46)}$$

Exponential Equation:

$$f(D) = a+b*\exp(-c*D); \quad f(0) = a+b \qquad \text{——— (47)}$$

[First Derivative]:

$$f'(D) = -bc*\exp(-c*D); \quad f'(0) = -bc \qquad \text{——— (48)}$$

[Second Derivative]:

$$f''(D) = bc^2*\exp(-c*D); \quad f''(0) = bc^2 \qquad \text{——— (49)}$$

(iii) Because the quadratic curve and the saturating

exponential curve approximate each other and the coefficients of the quadratic equation, r_1, r_2 and r_3 are known; the coefficients of the saturating exponential equation ('a', 'b' and 'c') can be found initially by equating the quadratic equations to the exponential equation and then by equating the first and second derivatives of the quadratic equation with the first and second derivatives of the exponential equation while at zero dose.

Therefore, equating equation (44) to (47), (45) to (48), and (46) to (49), the values of parameters 'a', 'b' and 'c' are calculated as follows:

$$a = r_1 - (r_2^2 / 2r_3)$$
$$b = (r_2^2 / 3r_3)$$
$$c = (-2r_3 / r_2).$$

4.2 MONTE CARLO SIMULATION

The quality of the estimation scheme discussed in Chapter Two will be studied by Monte Carlo simulation in this section. This study will be outlined in the following sections:

4.2.1 DESIGN OF MONTE CARLO STUDY

4.2.2 ESTIMATION OF THE PARAMETERS

and 4.2.3 NOMINAL CONFIDENCE LEVEL VERSUS OBSERVED CONFIDENCE LEVEL OF PARAMETERS AND INTERSECTION POINTS.

4.2.1 DESIGN OF MONTE CARLO STUDY

Five sets of Monte Carlo data sets were generated as follows:

[SET 1]: a set of 2000 data sets each of size 12 with parameter values 'a'=8, 'b'=-6, 'c'=2 and σ=0.03.

[SET 2]: a set of 2000 data sets each of size 24 with parameter values 'a'=8, 'b'=-6, 'c'=2 and σ=0.03.

[SET 3]: a set of 1000 data sets each of size 16 (data set 1A of sample QNL84-1) with parameter values 'a'=10.805539, 'b'=-7.933527, 'c'=2.306339 and σ=0.053371.

[SET 4]: a set of 1000 data sets each of size 14 (data set 1B of sample QNL84-1) with parameter values 'a'=6.297899, 'b'=-4.486734, 'c'=1.854243 and σ=0.04993506.

[SET 5]: a set of 1000 data sets each of size 11 (data set 1C of sample QNL84-1) with parameter values 'a'=2.695834, 'b'=-1.887451, 'c'=1.565947 and σ=0.05599857.

The parameter values for the first two sets were rounded off versions based on a suggestion by Dr. G. Berger. (These parameter values used to generate random numbers will be referred to as the true parameter values.) The remaining three sets of parameter values are the fitted values for data sets 1A, 1B and 1C analysed in Chapter Five.

The above five sets of Monte Carlo data sets were generated based on the saturating exponential model. The saturating exponential model of equation (3) can be rewritten as follows:

$$Y_i = [a+b*\exp(-cx_i)]*(1+\sigma\epsilon_i) \qquad \text{——— (50).}$$

The error terms of equation (50), ϵ_i, are independently identically distributed N(0,1) (i.i.d. N(0,1)). Because each ϵ_i is an i.i.d. N(0,1) random number, artificial N(0,1) random numbers were simulated by an IMSL routine called GGNML. From the simulated N(0,1) random numbers of a given sample size, the true parameters, 'a', 'b' and 'c', and the given values of the independent variable (the applied doses), the values of the dependent variable (the TL intensities), were calculated by equation (50).

In spite of the fact that the range of experimental sample sizes given for the R-Γ is from 11 to 17, Monte Carlo data sets each of sizes 12 and 24 were generated. The results in Table 4.2.2 show that the estimated standard errors of size 12 is larger than which of size 24 by a factor of approximately $\sqrt{2}$ as expected.

The estimated intersection points, at which the saturating exponential curve and the x-axis cross, are calculated for each Monte Carlo data set by the following equation:

$$\hat{x}^* = (-1/\hat{c})*\ln(-\hat{a}/\hat{b}) = f(\hat{a},\hat{b},\hat{c}),$$

where, $\hat{x}^*$ is the estimated intersection point;

$\hat{a}$, $\hat{b}$ and $\hat{c}$ are the estimated parameters.

2000 intersection points were calculated for each of the first two Monte Carlo data sets and 1000 intersection points were calculated for each of the remaining three sets. These calculations were done by FORTRAN programs CONFIFIS4, CONFIFIS4-24, CONFIFIS4A, CONFIFIS4B and CONFIFIS4C (APPENDIX A).

4.2.2 ESTIMATION OF THE PARAMETERS

The saturating exponential model (equation (3)) was fitted to each of the five Monte Carlo data sets by the IRLS algorithm using the BMDP3R program. The true parameter values were used for the initial estimates to feed to the BMDP3R program. The BMDP3R output produces values for the Asymptotic Correlation Matrix of the Parameters, Residual Mean Square, Degree of Freedom, the Estimated Parameters (IRLS estimates) and their associated Asymptotic Standard Deviations. A sample BMDP3R output is displayed on the following page. The asymptotic standard deviations produced by BMDP are not strictly appropriate since they appear to be based on the assumption that the weights are known.

The average IRLS estimates (the Monte Carlo estimates) and the estimated standard errors (the SD is the SD of the Monte Carlo estimates) obtained from the theoretical

variance-covariance matrices are summarized in Table 4.2.2 for each set of Monte Carlo data sets. In this table, the average IRLS estimate of Monte Carlo data sets [SET 1] (n=12) and [SET 2] (n=24) are the average of the 2000 IRLS estimates while [SET 3] (1A), [SET 4] (1B) and [SET 5] (1C) are the average of the 1000 IRLS estimates. The Monte Carlo standard errors are the root mean square errors of the Monte Carlo values about the true parameter values. If our asymptotic theory is working well these SE's should be close to the values labelled asymptotic standard error which are computed using the formular of Chapter Two and Three.

ASYMPTOTIC CORRELATION MATRIX OF THE PARAMETERS

		P1	P2	P3
		1	2	3
P1	1	1.0000		
P2	2	-0.9835	1.0000	
P3	3	-0.8753	0.8374	1.0000

RESIDUAL MEAN SQUARE 0.588612E-03

DEGREES OF FREEDOM 9

PARAMETER	ESTIMATE	ASYMPTOTIC STANDARD DEVIATION	TOLERANCE
P1	7.889383	0.154078	0.0237842773
P2	-5.878509	0.154078	0.0303805494
P3	2.012553	0.110435	0.2170771782

The entries of the (4x4) Fisher information matrix are calculated by the formula given in section 2.2.4 of Chapter Two. The (4x4) theoretical variance-covariance matrix is then obtained by inverting this Fisher information matrix. The theoretical variances of the estimates are the diagonal entries of this theoretical variance-covariance matrix. Then the theoretical standard deviations are obtained by taking the square roots of their theoretical variances. FORTRAN programs called CONFIFIS4, CONFIFIS4-24, CONFIFIS4A, CONFIFIS4B and CONFIFIS4C (APPENDIX A) were written to calculate the elements of the Fisher information matrix and the theoretical variance-covariance matrix.

	ESTIMATES	MONTE CARLO DATA SETS				
		SET 1	SET 2	SET 3	SET 4	SET 5
INITIAL PARAMETER VALUES	a	8	8	10.80554	6.29790	2.69583
	b	-6	-6	-7.93353	-4.48673	-1.88745
	c	2	2	2.30634	1.85424	1.56595
	sigma	0.03	0.03	0.05337	0.04994	0.05600
AVERAGE IRLS ESTIMATES	a	8.00496	8.00899	10.82079	6.32307	2.71231
	b	-6.00654	-6.01036	-7.94777	-4.51339	-1.90191
	c	2.00182	1.99860	2.30838	1.85193	1.58331
	sigma	0.02870	0.02888	0.05210	0.04892	0.05431
MONTE CARLO STANDARD ERROR	a	0.19393	0.19040	0.24690	0.16220	0.11464
	b	0.19510	0.19125	0.24796	0.16240	0.11299
	c	0.13052	0.12675	0.16280	0.13924	0.17581
	sigma	0.00695	0.00698	0.00729	0.00744	0.01000
ASYMPTOTIC STANDARD ERROR	a	0.19220	0.13714	0.23819	0.16237	0.11208
	b	0.19209	0.13705	0.24014	0.16269	0.11119
	c	0.13280	0.09430	0.16044	0.14096	0.17391
	sigma	0.00603	0.00429	0.00667	0.00671	0.00850

[Table 4.2.2] The average IRLS estimates (the Monte Carlo estimates), Monte Carlo standard errors and asymptotic standard errors of all five Monte Carlo data sets described in section 4.2.1.

4.2.3 NOMINAL CONFIDENCE LEVEL VERSUS OBSERVED CONFIDENCE LEVEL

The interval $[\hat{\theta} \pm \hat{\sigma}_{\hat{\theta}} * t_{\nu,(\alpha/2)}]$ is supposed to be a level $(1-\alpha)$ C.I. (nominal confidence level). Its real confidence level can be estimated from the Monte Carlo results by taking

$$\frac{\left[\begin{array}{c}\text{number of simulations} \\ \text{such that} \\ \text{equation (51) is satisfied}\end{array}\right]}{[\text{total number of simulations}].}$$

Where equation (51) is as follows:

$$| \hat{\theta} - \theta | \leq t_{\nu,(\alpha/2)} * \hat{\sigma}_{\hat{\theta}} \qquad \text{(51)}$$

where, θ = True parameters, 'a', 'b', and 'c';

$\hat{\theta}$ = Estimated parameters, $\hat{a}$, $\hat{b}$, and $\hat{c}$ (the IRLS estimates);

$t_{\nu,(\alpha/2)}$ = t-distribution critical point with a degree of ν freedom of (sample size - number of parameters estimated) and upper tail area $(\alpha/2)$;
(It should be noted that the t-distribution critical point is used because variance of the estimated parameter $\hat{\theta}$ is estimated.)

$\hat{\sigma}_{\hat{\theta}}$ = The theoretical standard deviation of estimated parameter $\hat{\theta}$.

The observed confidence level based on equation (51) has an SD

of

$$\sqrt{[a*(1-a)/1000]} * 100\%.$$

FORTRAN programs CONFIFIS4, CONFIFIS4-24, CONFIFIS4A, CONFIFIS4B and CONFIFIS4C (APPENDIX A) were written to compute various observed confidence levels with the theoretical standard deviations. The theoretical standard deviations are the square roots of the diagnol entries of the theoretical variance-covariance matrix. The standard deviation at the estimated intersection point is obtained as follows:

The intersection point with the x-axis can be obtained by solving the following equations,

$$a+b*\exp(-cx^*) = 0$$

$$\hat{a}+\hat{b}*\exp(-\hat{c}\hat{x}^*) = 0$$

where, 'a', 'b' and 'c' are the true parameters;

$\hat{a}$, $\hat{b}$ and $\hat{c}$ are the estimated parameters.

The roots of these equations are as follows:

$$x^* = (-1/c)*\ln(-a/b) = f(a,b,c)$$
$$\hat{x}^* = (-1/\hat{c})*\ln(-\hat{a}/\hat{b}) = f(\hat{a},\hat{b},\hat{c}) \qquad \text{——— (52).}$$

Because $(\hat{x}^*-x^*)$ is normally distributed as follows (Chapter Three):

$$(\hat{x}^*-x^*) \sim N(0,\nabla f^T I'\nabla f)$$

where, $\nabla f^T = (\partial f/\partial \hat{a}, \partial f/\partial \hat{b}, \partial f/\partial \hat{c})$;

I' is the same as those in Chapter Three;

the standard deviation of $(\hat{x}^*-x^*)$ is $\sqrt{\nabla f^T I' \nabla f}$. Therefore, the observed confidence level of the intersection point is estimated the same as that of parameters. Where, equation (51) becomes as follows:

$$| \hat{x}^*-x^* | \leq t_{\nu,(\alpha/2)} * \sqrt{\nabla f^T I' \nabla f}.$$

Various nominal confidence levels and observed confidence levels of parameters 'a', 'b', 'c' and $\hat{x}$ for all five Monte Carlo data sets are summarized in Table 4.2.3 of the following page.

MONTE CARLO DATA SETS	PARAMETERS AND INTERSECTION POINTS	NOMINAL CONFIDENCE LEVELS (%)	OBSERVED CONFIDENCE LEVELS (%)
SET 1(n=12)	a	97.5	97.75
		95.0	95.0
		75.0	72.9
	b	97.5	98.0
		95.0	94.35
		75.0	73.1
	c	97.5	97.8
		95.0	96.4
		75.0	75.45
	x	97.5	97.8
		95.0	95.2
		75.0	75.4
SET 2(n=24)	a	97.5	96.8
		95.0	94.75
		75.0	74.55
	b	97.5	96.65
		95.0	93.9
		75.0	74.7
	c	97.5	96.55
		95.0	93.35
		75.0	74.8
	x	97.5	96.55
		95.0	93.9
		75.0	73.9

MONTE CARLO DATA SETS	PARAMETERS	NOMINAL CONFIDENCE LEVELS (%)	OBSERVED CONFIDENCE LEVELS (%)
SET 3 (1A)	a	97.5	97.3
		95.0	94.0
		75.0	74.2
	b	97.5	97.5
		95.0	94.4
		75.0	74.2
	c	97.5	96.7
		95.0	94.2
		75.0	73.4
	x	97.5	97.9
		95.0	95.2
		75.0	74.9
SET 4 (1B)	a	97.5	97.6
		95.0	95.3
		75.0	76.8
	b	97.5	97.6
		95.0	96.2
		75.0	76.4
	c	97.5	97.6
		95.0	95.2
		75.0	76.6
	x	97.5	98.0
		95.0	95.7
		75.0	77.0
SET 5 (1C)	a	97.5	97.3
		95.0	95.7
		75.0	73.3
	b	97.5	97.8
		95.0	95.2
		75.0	72.8
	c	97.5	96.7
		95.0	94.5
		75.0	76.1
	x	97.5	97.6
		95.0	94.7
		75.0	75.9

[Table 4.2.3] Various observed confidence levels of parameters and the intersection points are listed to compare with their nominal confidence levels for all five Monte Carlo data sets described in section 4.2.1.

4.3 SUMMARY

To fit a non-linear saturating exponential model with a weight which is a function of its coefficients (parameters), initial parameter estimates are required to proceed with the IRLS algorithm using the BMDP3R program. These initial parameters can be obtained by a Graphical Method or a Quadratic Equation Method. The estimation scheme, using the IRLS estimates and the theoretical standard deviations calculated by the MLE theory, is then examined by Monte Carlo study. Estimated variances are then calculated by the MLE theory using the theoretical variances obtained from the diagonal entries of theoretical variance-covariance matrix.

The intersection point x^* based on the MLE theory applied to the IRLS estimates or MLEs discussed here have true coverage probability close to the nominal coverage probability. The quality of these approximations is improved by using t-distribution critical points instead of normal distribution critical points as explained in Chapter Three.

CHAPTER 5

ANALYSIS OF EXPERIMENTAL DATA

Five different sediment samples, classified as QNL84-1, QNL84-2, QNL84-3,5W, QNL84-4, QNL84-3,12, underwent the R-Γ procedure. For each sediment sample there were three data sets collected, data set A, data set B and data set C. The actual data are in APPENDIX B. Data set A is the thermoluminescence signal observed for the unbleached sediments, data set B is for bleached sediments, and data set C is for sediments bleached for a longer time than data set B. They are plotted on the same diagram of TL versus applied dose. Two intersection points are extrapolated from these three curves on the same diagram. The saturating exponential model with constant percent error was fitted to each data set. The IRLS estimates and their theoretical standard deviations are shown in section 5.1. In section 5.2 both intersection points of each sediment sample are calculated by the IMSL routine ZBRENT and their standard errors are calculated. To conclude, the validity of the constant percent error assumption and the adequacy of the saturating exponential model will be examined in section 5.3. Finally, the results of the analyses of the experimental data will be summarized in section 5.4.

5.1 ESTIMATION OF PARAMETERS BY ITERATIVELY REWEIGHTED LEAST SQUARES

As mentioned in Chapter Two when σ is small the IRLS estimation scheme is the same as the MLE estimation scheme. For each experimental data the IRLS estimates are sought in this section. To obtain the IRLS estimates the initial parameter values, 'a'=2, 'b'=-8, 'c'=6, and 'σ'=0.03 were entered into the BMDP3R program. The IRLS estimates produced by the BMDP and their theoretical standard deviations are listed in Table 5.1. These theoretical standard deviations for each of the data sets were computed by entering the IRLS estimates into FORTRAN programs EFISHER4*4-1, EFISHER4*4-2, EFISHER4*4-3, EFISHER4*4-4 and EFISHER4*4-5.

	SAMPLE	1			2			3		
	ESTIMATES	A	B	C	A	B	C	A	B	C
IRLS ESTIMATES	a	10.8055	6.2979	2.6958	14.2804	9.6575	4.5778	4.3874	2.3787	1.3846
	b	-7.9335	-4.4867	-1.8874	-10.4415	-7.4946	-3.4004	-3.8623	-2.0164	-1.1340
	c	2.3063	1.8542	1.5659	2.5508	1.3095	1.3777	2.8438	2.3548	2.1431
THEORETICAL STANDARD DEVIATIONS	a	0.3380	0.3973	0.1516	0.5767	1.1963	0.2878	0.2493	0.1346	0.0663
	b	0.3382	0.3906	0.1514	0.5694	1.1870	0.2859	0.2492	0.1346	0.0650
	c	0.1813	0.1485	0.1178	0.1811	0.2133	0.1143	0.1680	0.1744	0.1510

	SAMPLE	4			5		
	ESTIMATES	A	B	C	A	B	C
IRLS ESTIMATES	a	6.3515	3.6480	2.1696	16.1886	7.0986	4.2585
	b	-4.2068	-2.4698	-1.5145	-14.1614	-5.8253	-3.4435
	c	2.0783	1.3592	1.4574	3.3110	2.5623	1.7398
THEORETICAL STANDARD DEVIATIONS	a	0.3305	0.5164	0.3466	0.4388	0.3851	0.9385
	b	0.3274	0.5117	0.3401	0.4376	0.3806	0.9332
	c	0.2951	0.2950	0.3429	0.1565	0.2101	0.3568

[Table 5.1] The IRLS estimates and their theoretical standard deviations of all five experimental data sets.

5.2 ESTIMATIONS OF THE INTERSECTION POINTS AND THEIR VARIANCES

The estimated intersection points of the TL response curves were computed using the IMSL algorithm ZBRENT. Their estimated variances were calculated by the maximum likelihood method (equation (37) in Chapter Two). The computations were incorporated into the programs EFIS4*4-1, EFIS4*4-2, EFIS4*4-3, EFIS4*4-4 and EFIS4*4-5. The results are displayed in Table 5.2 of the following page.

The estimated standard deviations at the estimated intersection point of two dose response curves for each sample shown in Table 5.2 range from 0.00100 (sample 3, data sets A and C) to 0.03885 (sample 4, data sets A and B). These estimated standard deviations enable the estimation of the TL apparent ages of the sediment samples to an accurate range.

It should be noted from Table 5.2 that the ED extrapolated from curves A and C is larger than that of curves A and B. Curve C was based on the subsamples bleached for longer periods. The standard error of the intersection point does not encompass the difference between the ED produced by these two intersection points. As stated in the Introduction it would be expected that this difference in ED would be within the range of the SE. This discrepancy is attributable to the fact that the sample was improperly zeroed (personal communication with Dr. Berger).

SAMPLE		1		2		3	
INTERCEPT CURVES		AB	AC	AB	AC	AB	AC
ESTIMATED INTERSECTION POINTS	x	-0.0936	-0.1163	-0.0864	-0.1045	-0.0250	-0.0306
	Y	0.9611	0.4314	1.2654	0.6512	0.2397	0.1737
ESTIMATED VARIANCES OF x		0.000241	0.000080	0.000200	0.000036	0.000007	0.000001
ESTIMATED STANDARD DEVIATIONS OF x		0.01552	0.00894	0.01414	0.00600	0.00265	0.00100
EQUIVALENT DOSE (ED)		0.09357	0.11630	0.08637	0.10445	0.02502	0.03062

SAMPLE		4		5	
INTERCEPT CURVES		AB	AC	AB	AC
ESTIMATED INTERSECTION POINTS	x	-0.1482	-0.1836	-0.0226	-0.0282
	Y	0.6271	0.1906	0.9255	0.6419
ESTIMATED VARIANCES OF x		0.001509	0.001072	0.000004	0.000004
ESTIMATED STANDARD DEVIATIONS OF x		0.03885	0.03274	0.00200	0.00200
EQUIVALENT DOSE (ED)		0.14821	0.18356	0.02263	0.02819

[Table 5.2] This table displays the estimated intersection points, their estimated variances, estimated standard deviations and the equivalent dose. (Equivalent dose (ED) is the absolute value of x-coordinate.)

5.3 DIAGNOSES OF THE STATISTICAL ANALYSIS OF THE EXPERIMENTAL DATA

In this section the assumption of constant percent error is assessed in section 5.3.1. As well, the adequecy of the model is examined in section 5.3.2.

5.3.1 CHECKING THE VALIDITY OF THE CONSTANT PERCENT ERROR ASSUMPTION

The standard deviation at each dose level can be estimated as follows:

$$SD = \sqrt{[\sum_{j=1}^{m}(TL_{ij}-\overline{TL}_i)^2]/(m-1)} \qquad \text{(53)}$$

where, TL_{ij} = The j^{th} TL measurement at dose level i;

$\overline{TL}_i$ = The average TL measurement at the i^{th} dose level;

$= (1/m)*\sum_{j=1}^{m}(TL_{i1}+ \cdots + TL_{im})$;

m = The number of TL measurements at dose level i.

For the assumption of constant percent error this standard deviation should be roughly equal to σ multiplied by the mean, $[a+b*\exp(-cx_i)]$ as follows:

$$SD = \sigma * \text{Mean}.$$

Plotting SD versus Mean should produce a straight line passing

through the origin with a constant slope of σ. For each data set the corresponding SD versus Mean scattered plots are shown in Figures 5.3.1(b), 5.3.1(c), 5.3.1(d), 5.3.1(e) and 5.3.1(f) on the following pages. In addition, the error bars are shown for the plots of the experimental data sets 5B and 3A. The plot of data set 5B is the most linear of all while the plot of 3A is curved at high mean values. Although data set 3A exhibits curvature, a straight line is still possible within the given error bars (95% C.I.) in Figure 5.3.1(a).

The error bars are constructed as follows:

Knowing that (SD^2/σ^2) has a chi-square distribution with a degree of freedom (m-1), a $(1-\alpha)$ confidence is then calculated as follows:

$$\sqrt{\{[(m-1)*SD^2]/\chi^2_{(\alpha/2),(m-1)}\}} \leq \sigma_i \leq \sqrt{\{[(m-1)*SD^2]/\chi^2_{(1-\alpha/2),(m-1)}\}}$$

where, σ_i = Standard deviation of TL at dose level i;

SD = Standard Deviation;

m = Number of data points at a given dose level i.

In Figures 5.3.1(b), 5.3.1(c), 5.3.1(d), 5.3.1(e) and 5.3.1(f), straight lines passing through the origin can usually be drawn inside the error bars. The linear lines passing through the origin suggest that the constant percent error assumption for the model is not unreasonable. No formal test of assumption has been applied.

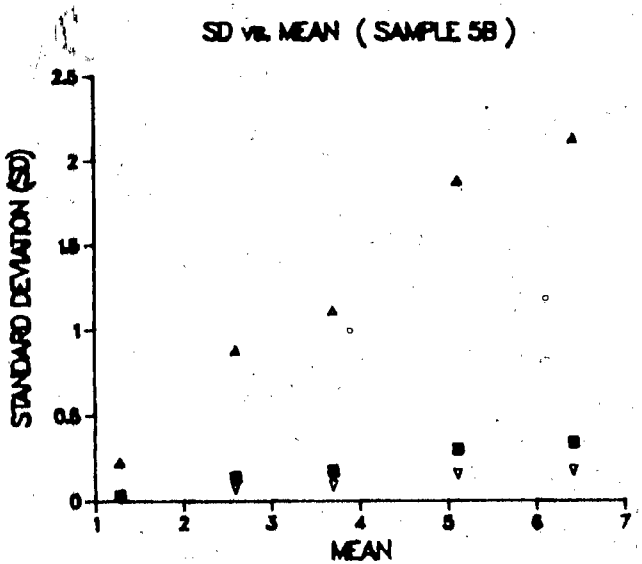

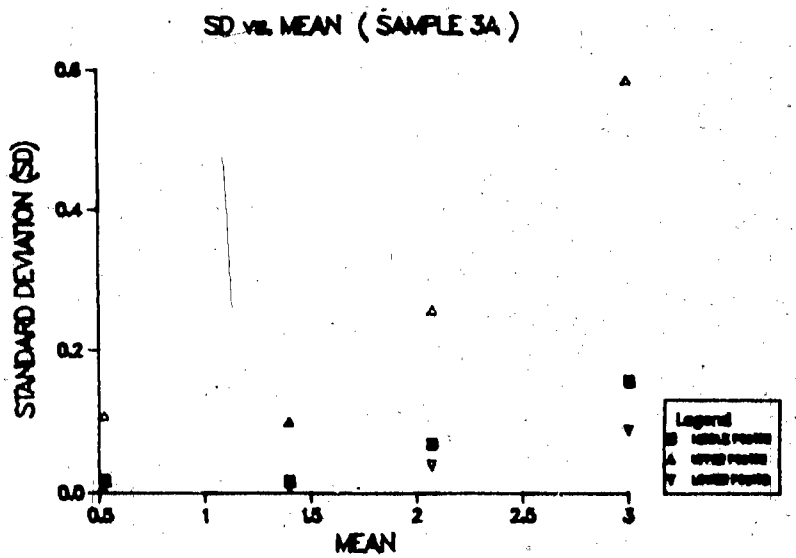

[Figure 5.3.1] The diagnosis of the constant percent error assumption.
[Figure 5.3.1 (a)] The plots of SD versus MEAN for experimental data sets 5B and 3A. The error bars are shown for the best straight line (sample 5B) and the worst straight line (sample 3A). It is obvious that curve 3A is curved at high mean values. However, straight line can still be drawn without exceeding the error bars for curve 3A.

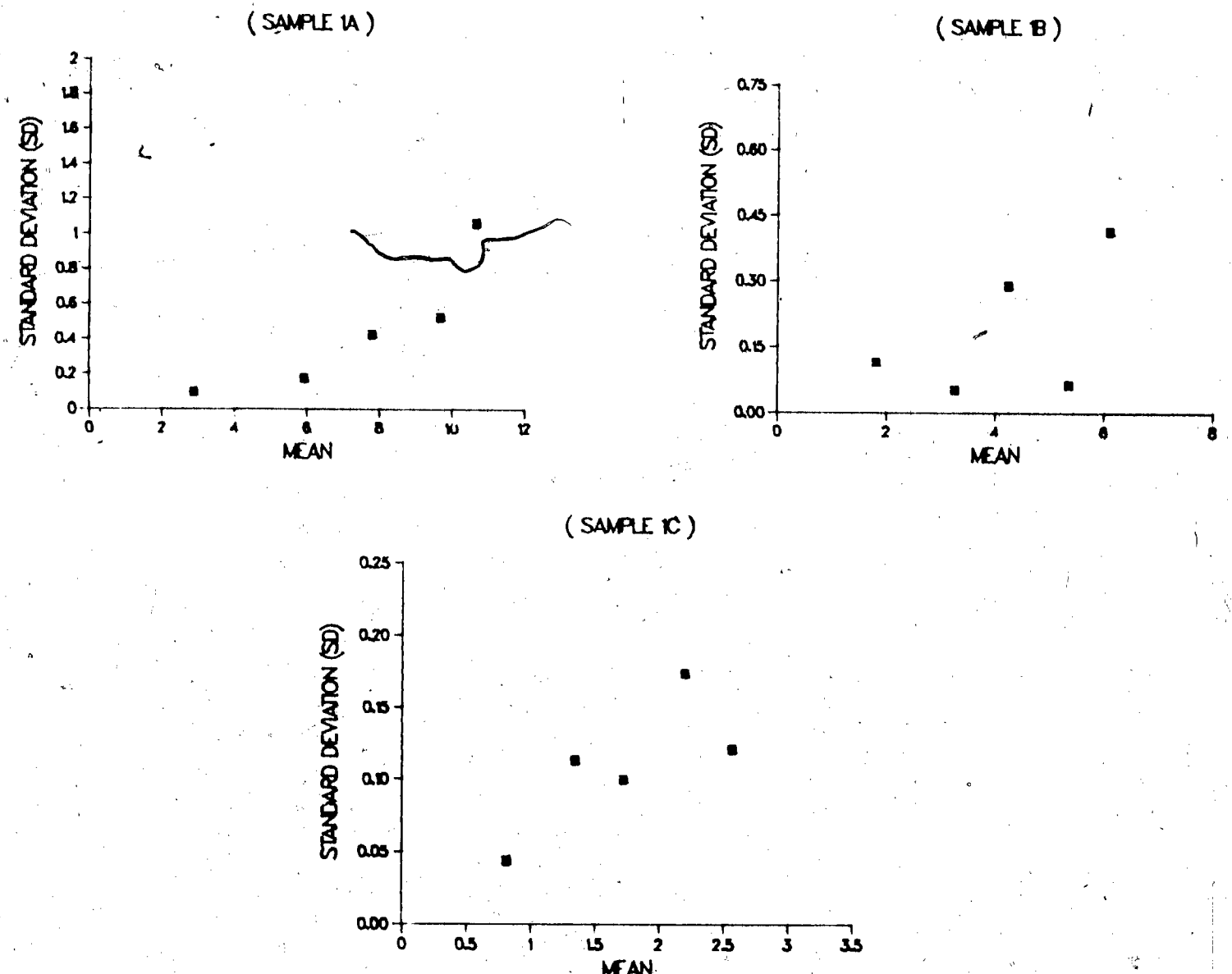

[Figure 5.3.1 (b)] The plots of SD versus Mean for experimental data sets 1A, 1B and 1C.

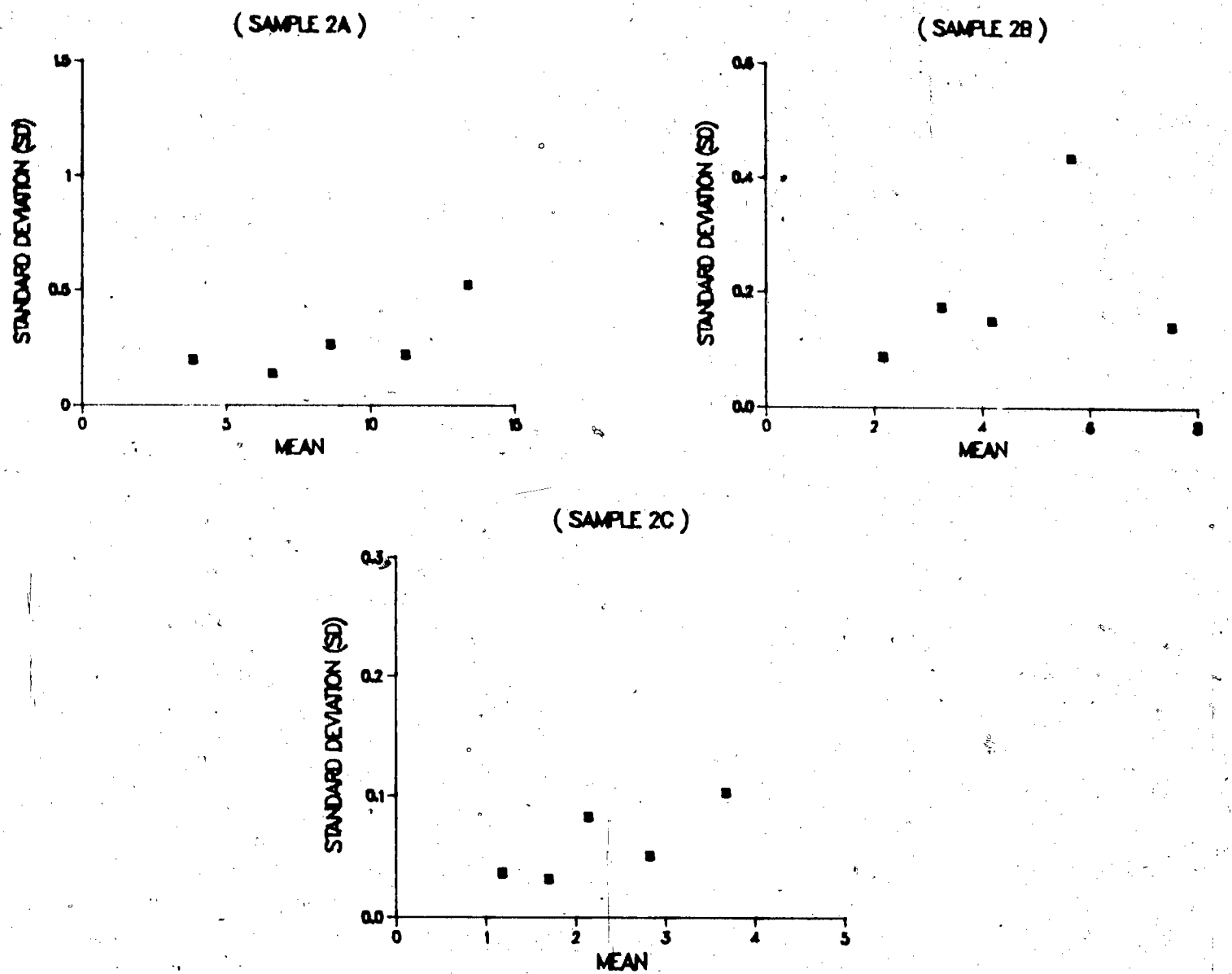

[Figure 5.3.1 (c)] The plots of SD versus Mean for experimental data sets 2A, 2B and 2C.

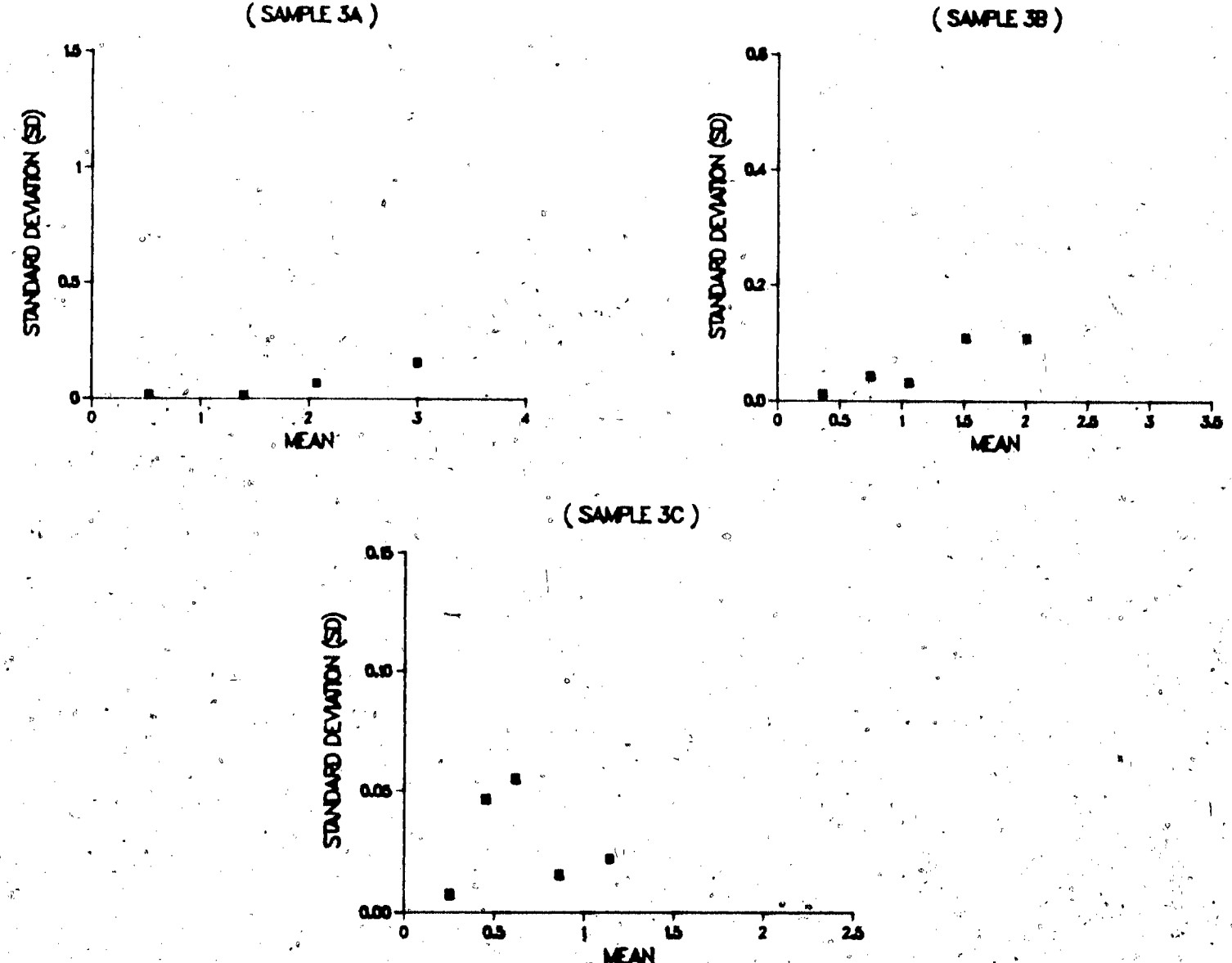

[Figure 5.3.1 (d)] The plots of SD versus Mean for experimental data sets 3A, 3B and 3C.

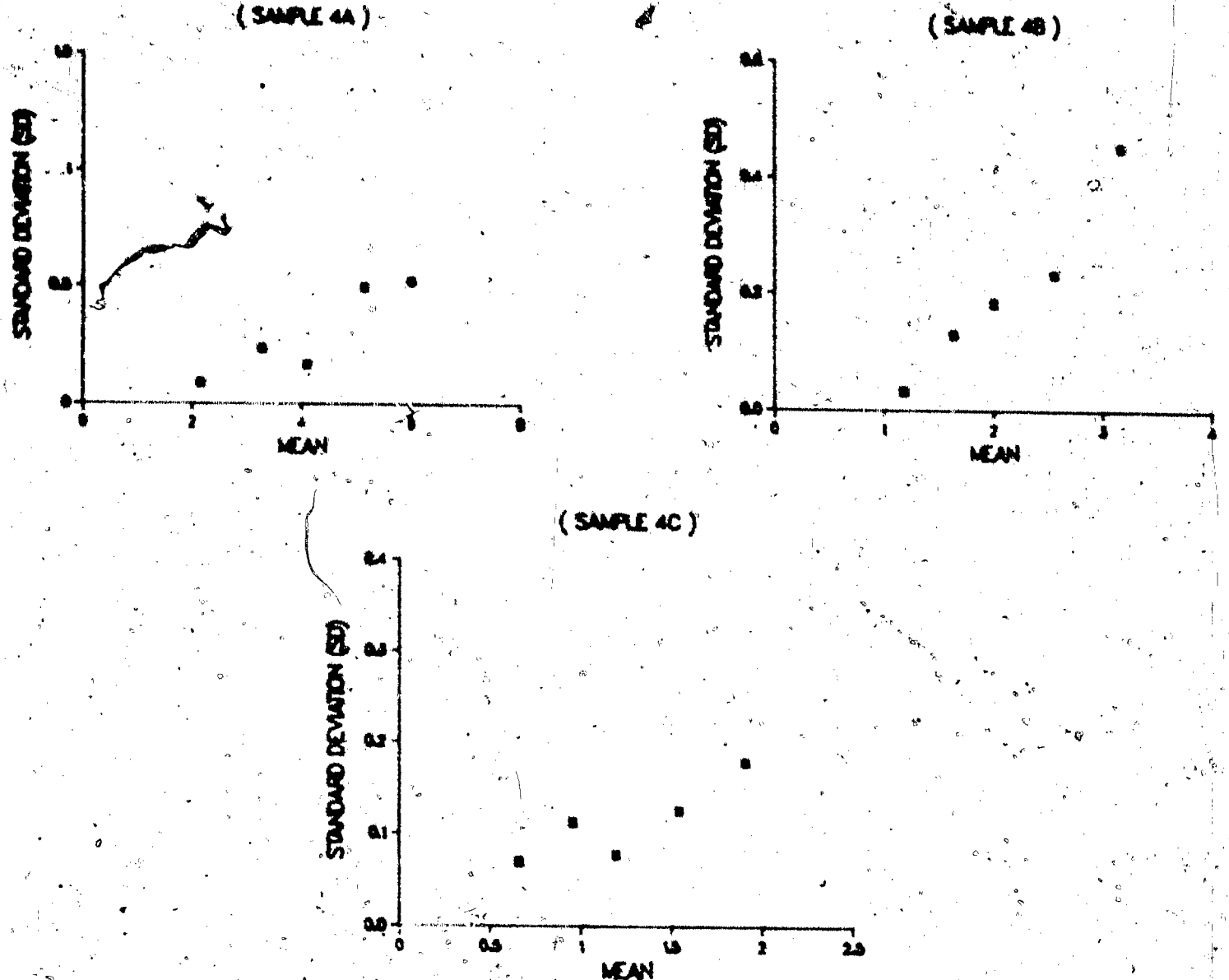

[Figure 5.3.1 (a)] The plots of SD versus Mean for experimental data sets 4A, 4B and 4C.

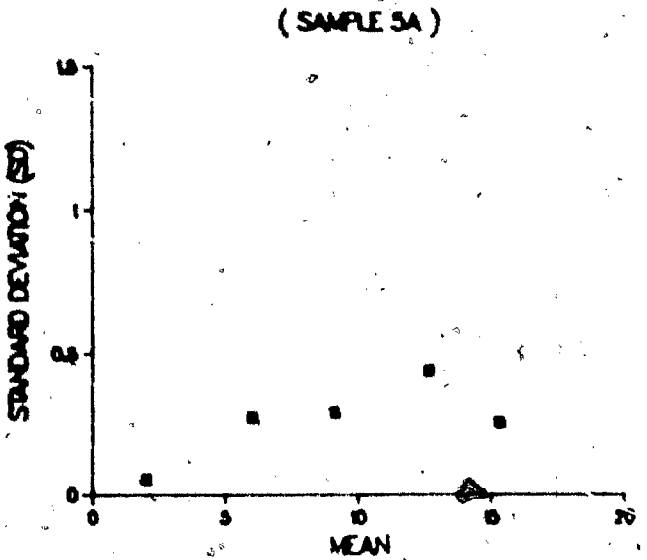

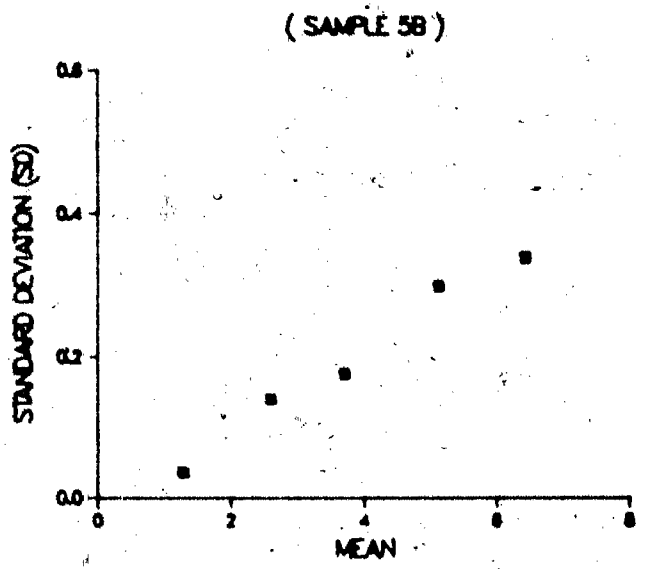

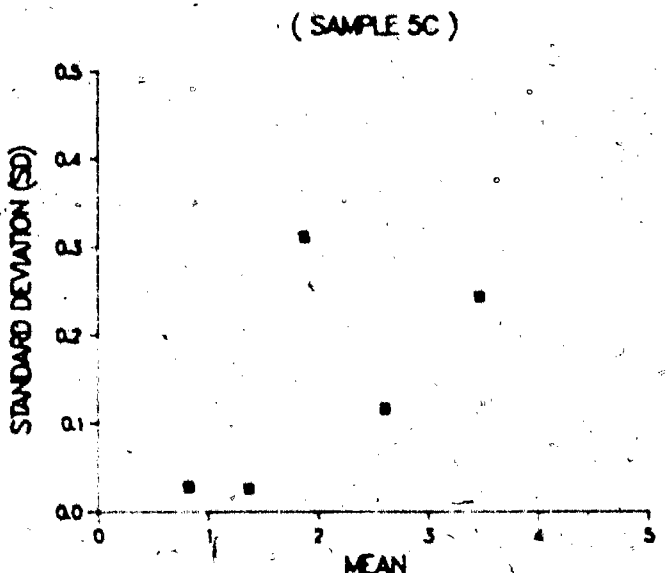

[Figure 5.3.1 (f)] The plots of SD versus Mean for experimental data sets 5A, 5B and 5C.

5.3.2 CHECKING THE ADEQUACY OF THE MODEL

If the saturating exponential model is appropriate and the assumptions of saturating exponential mean and constant percent error are satisfied, the residuals should be structureless. This may be examined by plotting the (Residual/Mean) versus the Mean for each data set. These plots are shown in Figures 5.3.2-1, 5.3.2-2, 5.3.2-3, 5.3.2-4 and 5.3.2-5 on the following pages. They are scattered randomly about the MEAN axis (x-axis). These pattern-free plots suggest that the model is adequate. It is noted that the data points are widely scattered along the vertical axis at each dose level. This is primarily due to selection of the vertical scale.

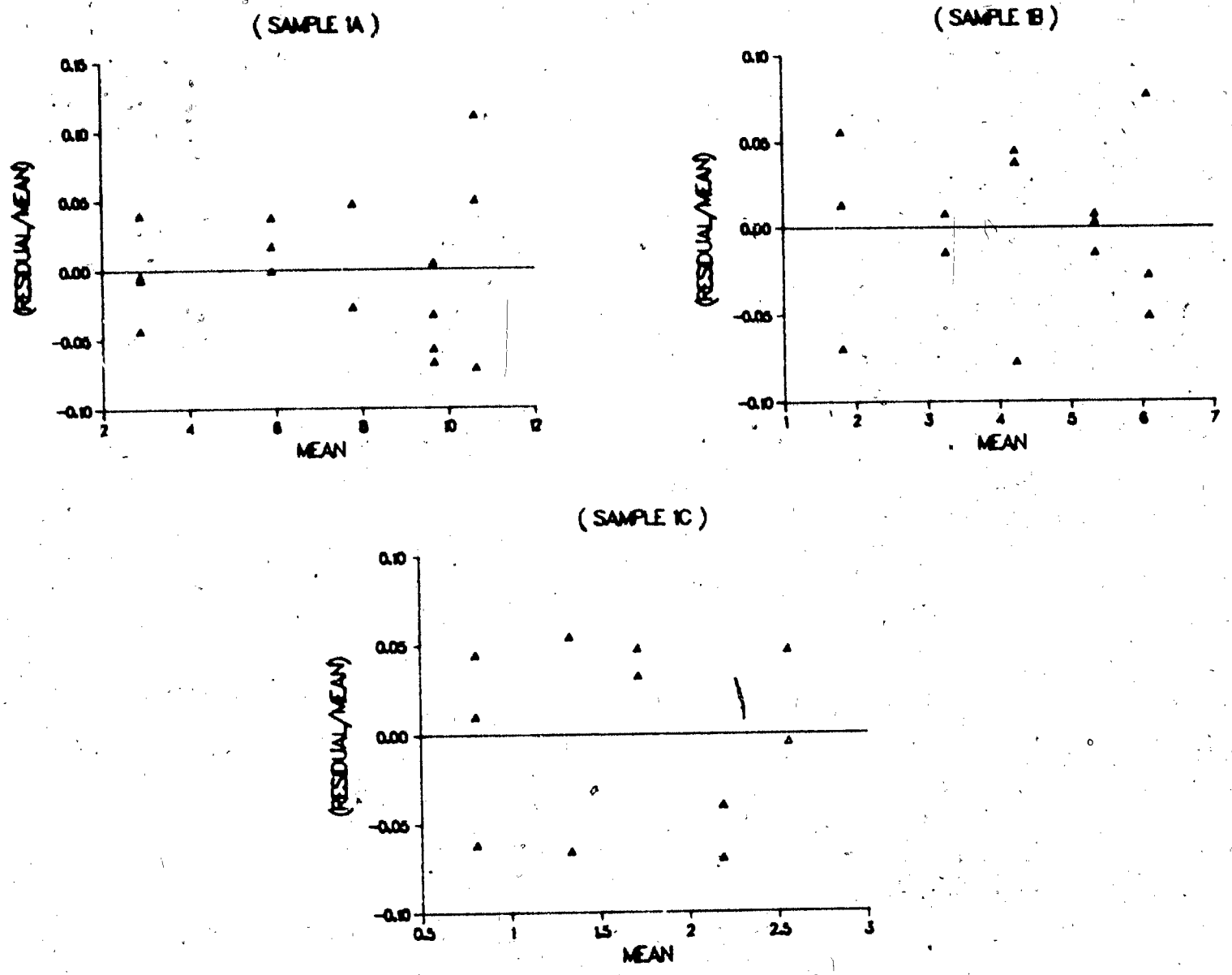

[Figure 5.3.2-1] The plots of (Residual/Mean) versus Mean for experimental data sets 1A, 1B and 1C.

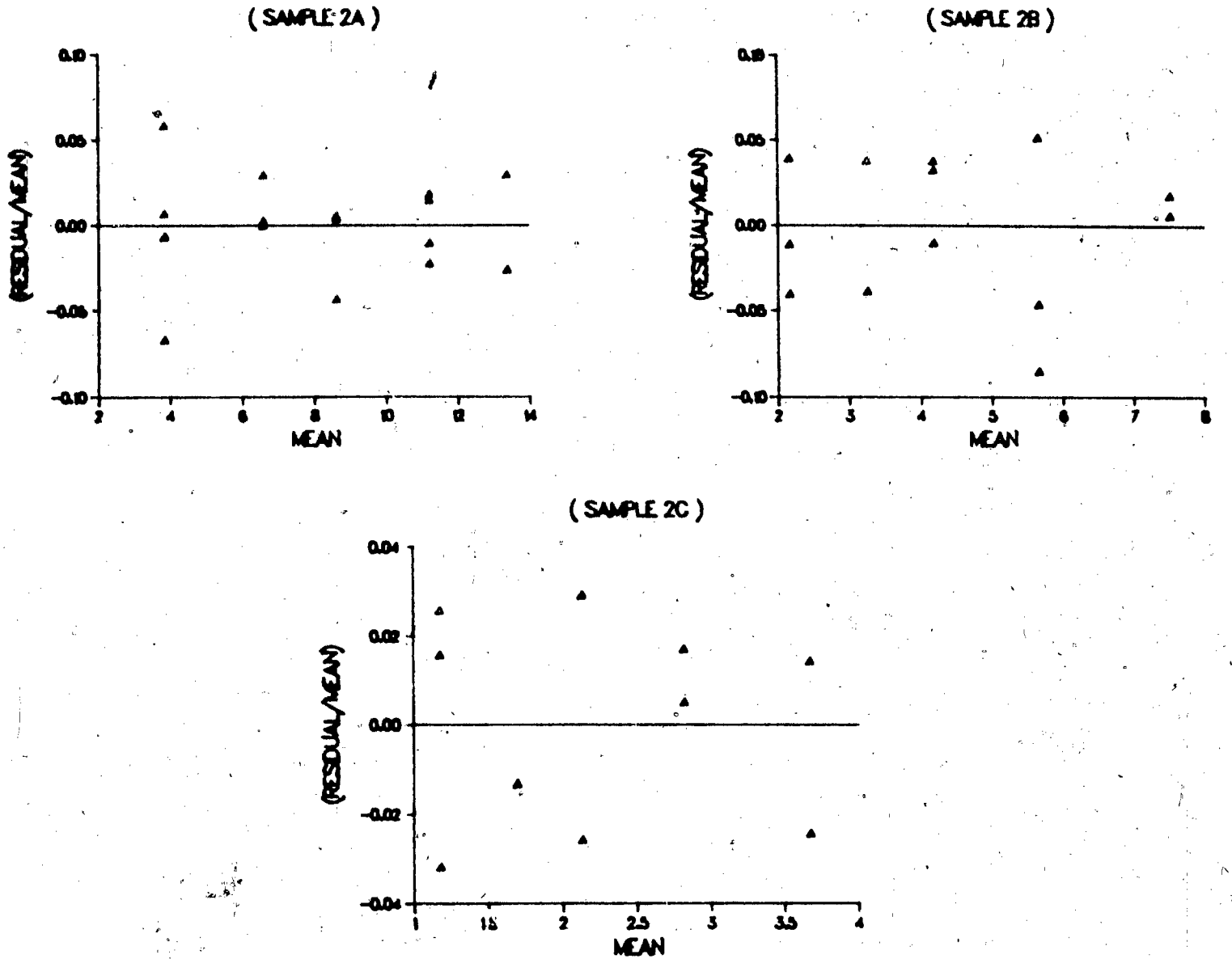

[Figure 5.3.2-2] The plots of (Residual/Mean) versus Mean for experimental data sets 2A, 2B and 2C.

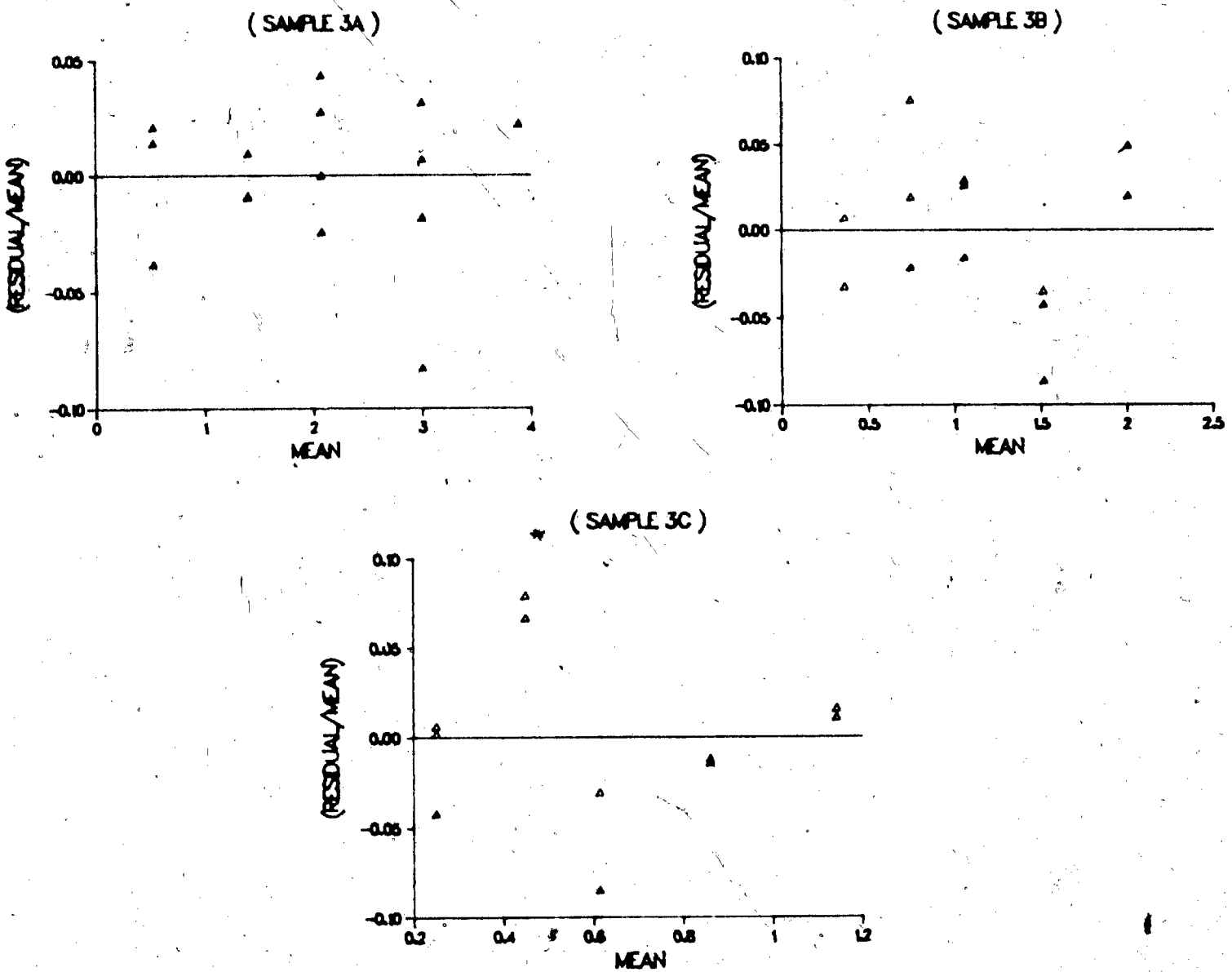

[Figure 5.3.2-3] The plots of (Residual/Mean) versus Mean for experimental data sets 3A, 3B and 3C.

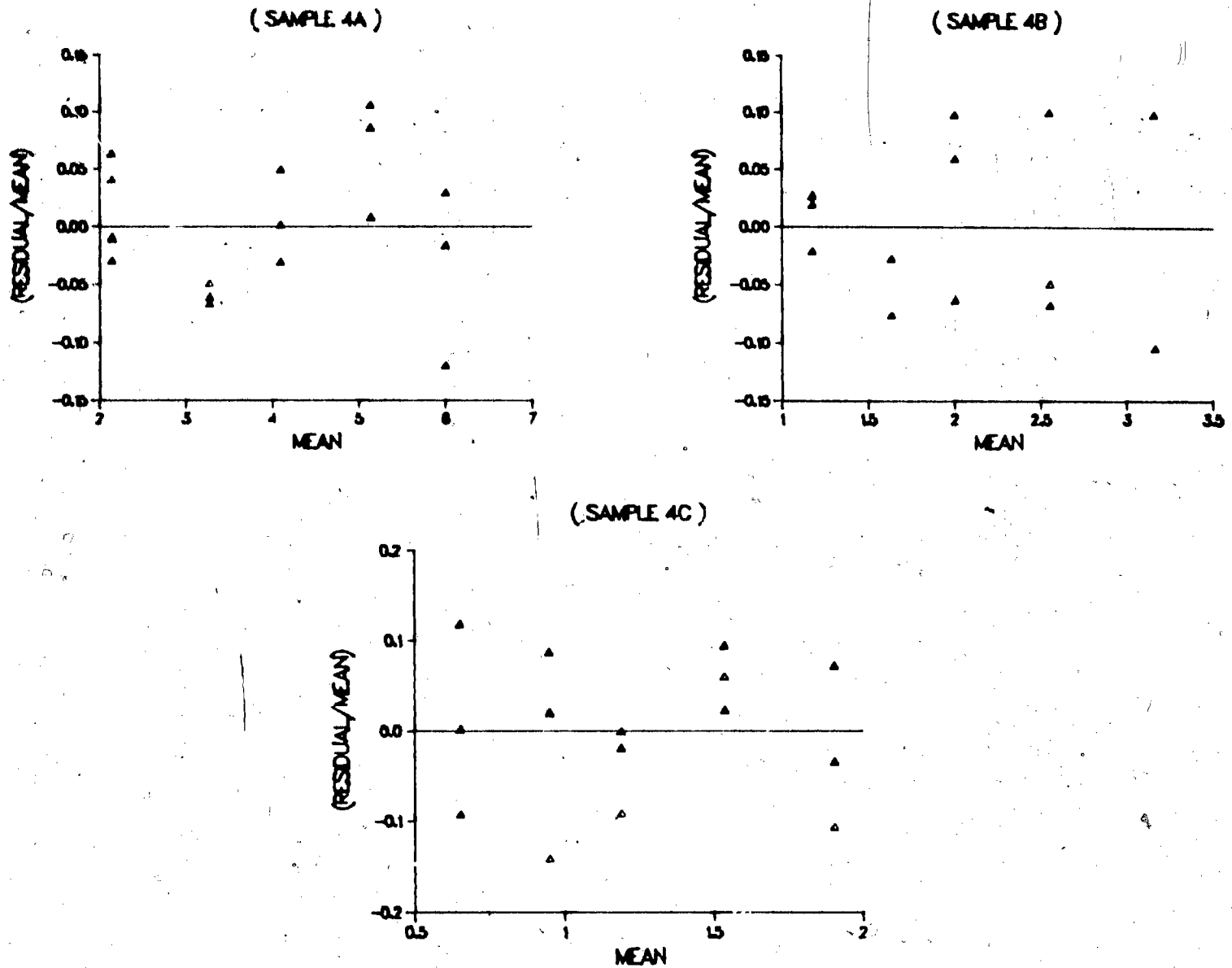

[Figure 5.3.2-4] The plots of (Residual/Mean) versus Mean for experimental data sets 4A, 4B and 4C.

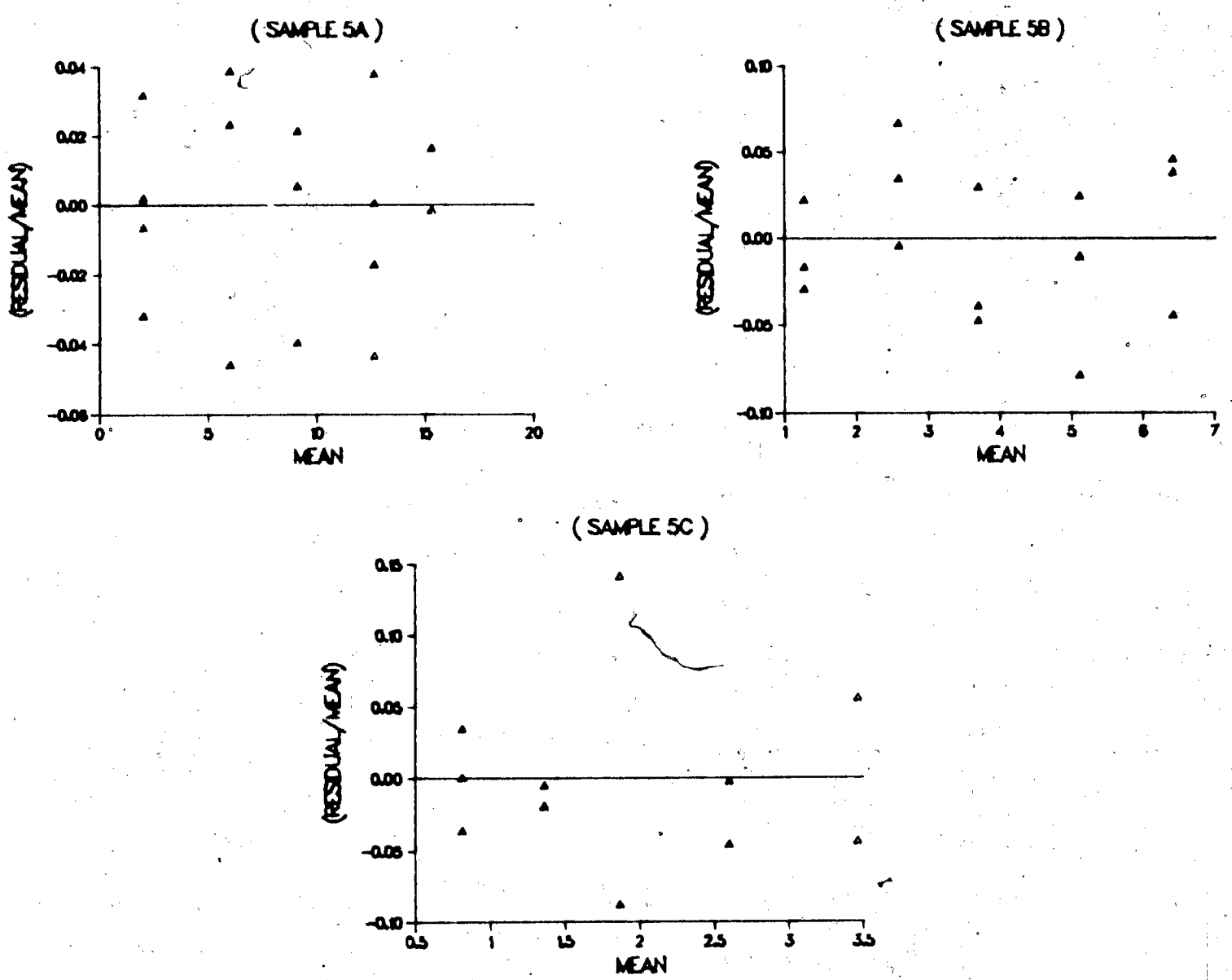

[Figure 5.3.2-5] The plots of (Residual/Mean) versus Mean for experimental data sets 5A, 5B and 5C.

5.4 SUMMARY

Incorporating the IRLS estimation scheme with the theoretical variances by the MLE theory, the estimated standard deviations of the intesection points are obtained for each sedimentary sample. The validity of the constant percent error assumption and the adequacy of the proposed saturating exponential model are examined by the plots of the SD versus the Mean and the (Residual/Mean) versus the Mean, respectively. The model appears to be adequate.

CHAPTER 6

SUGGESTIONS FOR FURTHER WORK

For a three dose response curve diagram, the saturating exponential model is fitted to each of data separately. This procedure yields three estimated parameters and one estimated σ (Chapter Five) for each dose response curve as well as two intersection points. Both these intersection points are functions of six estimated parameters (three from each curve). This condition results in an estimated variance of intersection points which is dependent on these estimated parameters as well as on the weights from both curves and the two estimated σ's. Other methods of fitting these data could be tried. For example, assuming that the two crossing TL response curves have the same percent errors, one could fit these two TL curves simultaneously. Possible physical reasons for assuming the same percent error for two crossing TL response curves are described in Berger et al. (1985). This method, while not actually carried out for this project, is described in this chapter.

When fitting two TL response curves at the same time with seven parameters, namely, 'a_A', 'b_A', 'c_A', 'a_B', 'b_B', 'c_B' and σ, the mean response appears as

$$Y_i = \{[a_A+b_A*\exp(-c_A x_i)]*(1+\sigma\epsilon_i\}*G + \{[a_B+b_B*\exp(-c_B x_i]*(1+\sigma\epsilon_i\}*(1-G) \qquad \text{(54)}$$

where, G=Indicator variable;

G=0 for data belong to A;

G=1 for data belong to B.

The IRLS estimates can be obtained the same way as that was described in Chapter Four where two curves were fitted separately.

The likelihood function for mean responses, $Y_1,\ldots,Y_n$, with a single σ for the two curves is as follows:

$$L = (1/\sqrt{2\pi}\sigma)^{(n_A+n_B)}*\{\exp(-1/2\sigma^2)*[\sum_{i=1}^{n_A}[Y_i-(a_A+b_A*\exp(-c_Ax_i))]^2 + \sum_{i=1}^{n_B}[Y_i-(a_B+b_B*\exp(-c_Bx_i))]^2]\} \quad \text{——— (55).}$$

The log likelihood function is shown as follows:

$$\begin{aligned} \ln L = {} & (-n_A/2)\ln(2\pi) - \sum_{i=1}^{n_A}(\ln\sigma) \\ & -(1/2)\sum_{i=1}^{n_A}[(Y_i-(a_A+b_A*\exp(-c_Ax_i)))/(\sigma(a_A+b_A*\exp(-c_AD)))]^2 \\ & + (-n_B/2)\ln(2\pi) - \sum_{i=1}^{n_B}(\ln\sigma) \\ & -(1/2)\sum_{i=1}^{n_B}[(Y_i-(a_B+b_B*\exp(-c_Bx_i)))/(\sigma(a_B+b*\exp(-c_Bx_i)))]^2 \end{aligned} \quad \text{——— (56).}$$

The Fisher information matrix is then a (7x7) matrix, I_{7x7} produced by overlapping σ terms from ${}_AI_{4x4}$ and ${}_BI_{4x4}$.

Where,

${}_AI_{4x4}$ = The Fisher Information matrix derived from equation (56). The four dimensions are parameters 'a_A', 'b_A', 'c_A', and σ;

${}_BI_{4x4}$ = The Fisher Information matrix derived from equation (56). The four dimensions are parameters 'a_B', 'b_B', 'c_B', and σ.

The theoretical variance-covariance matrix, $I^{-1}_{(7x7)}$ is the inverse of the Fisher information matrix, $I_{(7x7)}$. The variance of the intersection point is then estimated by equation (37) (shown in Chapter Three) with a (7x7) variance-covariance matrix and a $(\nabla f)^T$ of the form as follows:

$$(\partial f/\partial \hat{a}_A,\ \partial f/\partial \hat{b}_A,\ \partial f/\partial \hat{c}_A,\ \partial f/\partial \hat{o},\ -\partial f/\partial \hat{a}_B,\ -\partial f/\partial \hat{b}_B,\ -\partial f/\partial \hat{c}_B).$$

[NOTE]: $\partial f/\partial \hat{o} = 0$.

The (7x7) Fisher information matrix is illustrated as follows:

$$I_{7x7} = \begin{bmatrix} I_1 & a & 0 \\ a^T & c & b^T \\ 0 & b & I_2 \end{bmatrix}$$

where, I_1 is the (3x3) upper left array of the ${}_A I_{4x4}$ matrix and has the following form:

$$\begin{bmatrix} E(-\partial^2 \ln L/\partial a_A^2) & E(-\partial^2 \ln L/\partial a_A \partial b_A) & E(-\partial^2 \ln L/\partial a_A \partial c_A) \\ & E(-\partial^2 \ln L/\partial b_A^2) & E(-\partial^2 \ln L/\partial b_A \partial c_A) \\ & & E(-\partial^2 \ln L/\partial c_A^2) \end{bmatrix};$$

I_2 is the (3x3) upper left array of the ${}_B I_{4x4}$ matrix and has the following form:

$$\begin{bmatrix} E(-\partial^2 \ln L/\partial a_B^2) & E(-\partial^2 \ln L/\partial a_B \partial b_B) & E(-\partial^2 \ln L/\partial a_B \partial c_B) \\ & E(-\partial^2 \ln L/\partial b_B^2) & E(-\partial^2 \ln L/\partial b_B \partial c_B) \\ & & E(-\partial^2 \ln L/\partial c_B^2) \end{bmatrix};$$

$$a = \begin{bmatrix} E(-\partial^2 \ln L/\partial \sigma_A \partial a_A) \\ E(-\partial^2 \ln L/\partial \sigma_A \partial b_A) \\ E(-\partial^2 \ln L/\partial \sigma_A \partial c_A) \end{bmatrix}; \qquad b = \begin{bmatrix} E(-\partial^2 \ln L/\partial \sigma_B \partial a_B) \\ E(-\partial^2 \ln L/\partial \sigma_B \partial b_B) \\ E(-\partial^2 \ln L/\partial \sigma_B \partial c_B) \end{bmatrix};$$

$$c = E(-\partial^2 \ln L/\partial \sigma_A^2) + E(-\partial^2 \ln L/\partial \sigma_B).$$

[NOTE]: $\sigma_A = \sigma = \sigma_A$ is the σ in the term of 'A' of equation (56);

$\sigma_B = \sigma = \sigma_B$ is the σ in the term of 'B' of equation (56).

CONCLUSION

This paper studies the statistical analysis of the partial bleaching method for thermoluminescence dating of sedimentary rock. The non-linear saturating exponential model with a saturating exponential mean and an unknown constant percent error was fitted to several sets of data. It was shown that when σ is relatively small, the Iteratively Reweighted Least Squares (IRLS) estimation scheme approximates the Maximum Likelihood (ML) estimation scheme. Therefore, a Monte Carlo study was applied to examine the applicability of the large sample theory of the IRLS estimation scheme when σ is small and the number of observations is small. The intersection point of two additive dose curves was extrapolated using an IMSL algorithm and in addition, the standard deviations at these intersection points were approximately estimated by maximum likelihood theory. These techniques were applied to several experimental data sets. Finally, the model assumptions were checked by the plots of SD versus Mean and (Residual/Mean) versus Mean. The characteristics of linearity passing through the origin shown in the plots of SD versus Mean indicated the appropriateness of the constant percent error assumption while the randomness shown in the plots of (Residual/Mean) versus Mean assured the adequacy of the proposed model.

With these techniques the equivalent dose value was computed accurately as the distance from the origin to the intersection

point (beyond the origin) of two additive dose curves. In addition, the estimated error of this intersection point was calculated by the maximum likelihood theory. The TL apparent age is then obtained by the equation shown in the Introduction (page 8).

APPENDIX A

FORTRAN programs FOR, CONFIFIS4, CONFIFIS4-24, CONFIFIS4A, CONFIFIS4B, CONFIFIS4C, EFISHER4*4-1, EFISHER4*4-2, EFISHER4*4-3, EFISHER4*4-4, EFISHER4*4-5, EFISHER4*4-A, EFISHER4*4-B, EFISHER4*4-C, EFISHER4*4-M, CONFICAL, CONFICAL-24, CONFICALA, CONFICALB, CONFICALC will be provided upon request. The mailing address for the request of these programs is as follows:

Jen-ni Kuo
Department of Mathematics and Statistics
Simon Fraser University
Burnaby, British Columbia,
Canada V5A 1S6

DATA SET 1			
APPLIED DOSE (kGY/MIN) (×100)	TL INTENSITIES (×100000 PHOTON COUNTS/°C)		
	A	B	C
0.00	2.98660	1.83600	0.81690
0.00	2.86100	1.91932	0.84480
0.00	2.85360	1.68590	0.75890
0.00	2.74920	---	---
2.10	6.14170	3.28540	1.25060
2.10	6.01780	3.21280	1.41060
2.10	5.91430	---	---
4.20	8.16500	4.43140	1.80070
4.20	7.58430	4.40130	1.77490
4.20	---	3.91370	---
8.40	9.10790	5.39730	2.03810
8.40	9.34940	5.27580	2.10280
8.40	9.70660	5.37210	---
8.40	9.01470	---	---
16.80	9.88440	5.93270	2.54920
16.80	11.82850	5.79140	2.68090
16.80	11.17080	6.57240	---

DATA SET 2			
APPLIED DOSE (kGY/MIN) (×100)	TL INTENSITIES (×100000 PHOTON COUNTS/°C)		
	A	B	C
0.00	3.86710	2.07660	1.20780
0.00	3.58360	2.13930	1.14020
0.00	4.06460	2.24930	1.19610
0.00	3.81490	---	---
1.20	6.59310	3.12900	1.67340
1.20	6.61330	3.37790	1.67330
1.20	6.78870	---	---
2.40	8.24960	4.14270	2.08000
2.40	8.67080	4.32210	2.19700
2.40	8.65800	4.34500	---
4.80	10.96520	5.95550	2.83760
4.80	11.09780	5.40130	2.87100
4.80	11.41920	5.18040	---
4.80	11.38070	---	---
9.60	13.77890	7.66130	3.72470
9.60	13.03730	7.57480	3.58290

DATA SET 3			
APPLIED DOSE (kGY/MIN) (×100)	TL INTENSITIES (×100000 PHOTON COUNTS/°C)		
	A	B	C
0.00	0.53649	0.36500	0.25116
0.00	0.50512	0.35084	0.24014
0.00	0.53289	---	0.25228
0.90	1.38438	0.73165	0.47953
0.90	1.38526	0.80454	0.48538
0.90	1.41133	0.76216	---
1.80	2.07292	1.08711	0.56177
1.80	2.02206	1.09015	0.59505
1.80	2.13072	1.04283	---
1.80	2.16339	---	---
3.60	3.09620	1.45160	0.85048
3.60	3.02176	1.38487	0.84833
3.60	2.94492	1.46294	---
3.60	2.75210	---	---
7.20	3.97849	2.04972	1.16062
7.20	---	2.10886	1.15489

DATA SET 4				DATA SET 5			
APPLIED DOSE (kGY/MIN) (×100)	TL INTENSITIES (×100000 PHOTON COUNTS/°C)			APPLIED DOSE (kGY/MIN) (×100)	TL INTENSITIES (×100000 PHOTON COUNTS/°C)		
	A	B	C		A	B	C
0.00	2.12692	1.21030	0.59481	0.00	2.03152	1.23676	0.84384
0.00	2.12227	1.20153	0.73320	0.00	1.96315	1.30184	0.81587
0.00	2.23275	1.15389	0.65648	0.00	2.09222	1.25267	0.78631
0.00	2.28152	---	---	0.00	2.01449	---	---
0.00	2.08184	---	---	1.00	5.74421	2.76540	1.33958
1.50	3.11202	1.58944	1.03576	1.00	6.16032	2.68092	1.35879
1.50	3.07356	1.51078	0.81819	1.00	6.25363	2.58009	---
1.50	3.05579	---	0.97212	2.10	9.32165	3.52376	1.70589
3.00	3.97416	2.12509	1.19168	2.10	9.17411	3.55662	2.31468
3.00	4.29988	2.20243	1.16971	2.10	8.76386	3.80965	---
3.00	4.10482	1.88035	1.08331	4.20	12.11643	4.71203	2.59633
6.00	5.18758	2.81202	1.63178	4.20	12.67215	5.06155	2.48283
6.00	5.58707	2.43077	1.57395	4.20	13.14713	5.24063	---
6.00	5.68895	2.38528	1.68395	4.20	12.44773	---	---
12.00	5.28912	3.47800	1.70472	8.40	15.56710	6.13961	3.31161
12.00	6.18352	2.83563	2.04463	8.40	15.28946	6.71931	3.65489
12.00	5.90878	---	1.84255	8.40	---	6.67064	---

BIBLIOGRAPHY

Berger, G.W. and Lockhart, R.A. (in Press), "Regression and error analysis applied to the response curves in Thermoluminescence dating," *J. Mathematical Geology.* [Introduction, 1.1]

Berger, G.W., Huntely, D.J. and Stipp, J.J. (1984), "Thermoluminescence studies on a ^{14}C-dated marine core," *Canadian Journal of Earth Sciences*, **21**, 1145-1150. [1.1, 1.2.2]

Bickel, P.J. and Doksum, K.A. (1977), *Mathematical Statistics*, Holden-Day Inc., San Francisco. [1.2.2]

BMDP (1985), *BMDP statistical software*, University of California Press, Berkeley, Los Angeles and London.

Brent, R.P. (1971), "An algorithm with guaranteed convergence for finding a zero of a function," *The Computer Journal 14(4)*, 422-425.

Cameron, J.R., Suntharalingam, N. and Kenney, G.N. (1968), *Thermoluminescence dosimetry*, The University of Wilconsin Press, Milwaukee and London. [Introduction]

Chatterjee, S., Price, B. (1977), *Regression analysis by example*, John Wiley & Sons, New York, London, Sydney, Toronto, 101-105. [1.2.1]

Divigalpitiya, W.M.R. (1982), "Thermoluminescence dating of sediments," M.Sc. thesis, Simon Fraser University. [Introduction]

Draper, N.R. and Smith, H. (1981), *Applied Regression Analysis*, 2nd ed., John Wiley & Sons, New York, 77-81. [2.1.3]

Fleming, S. (1979), *Thermoluminescence techniques in archaeology*, Clarendon Press,Oxford. [Introduction]

Huntley, D.J. (1985), "On the zeroing of the thermoluminescence of sediments," *Physics and Chemistry of Minerals*, **12**, 122-127. [1.1]

IMSL (1982), *IMSL library reference manual*, 9th ed., IMSL Customer Relations, NBC Building, 7500 Bellaire Boulevard, Houston, Texas.

McDougall, D.J. (1968), *Thermoluminescence of geological materials*, Academic Press, London and New York. [Introduction]

Mckinlay, A.F. (1981), *Thermoluminescence dosimetry*, Adam Hilger Limited. [Introduction]

Neter, J., Wasserman, W. and Kutner, M.H. (1985), *Applied linear statistical models*, Richard D. Irwin, Inc. Homewood, Illinois 60430, 472-479. [2.1.3]

Ralston, M.L., Jennrich, R.I., Sampson, P.F. and Uno, F.K. (1979), "Fitting pharmacokinetic models with BMDPAR," *BMDP Technical Report No. 58, BMDP Statistical Software.*

Serfling, R.J. (1980), *Approximation theorems of mathematical statistics*, John Wiley & Sons, New York, 143-149. [3.2, 4.2.3, Chapter 6]

Wintle, A.G. and Huntley, D.J. (1982), "Thermoluminescence dating of sediments," *Quaternary Science Reviews*, 1, 31-53. [Introduction]

Aitken, M.J. (1985), *Thermoluminescence dating*, Academic Press. [Introduction]

INDEX